ADVANCED MATERIALS
www.advmat.de

Voltage-Control of Magnetism in All-Solid-State and Solid/Liquid Magnetoelectric Composites

Alan Molinari, Horst Hahn, and Robert Kruk**

The control of magnetism by means of low-power electric fields, rather than dissipative flowing currents, has the potential to revolutionize conventional methods of data storage and processing, sensing, and actuation. A promising strategy relies on the utilization of magnetoelectric composites to finely tune the interplay between electric and magnetic degrees of freedom at the interface of two functional materials. Albeit early works predominantly focused on the magnetoelectric coupling at solid/solid interfaces; however, recently there has been an increased interest related to the opportunities offered by liquid-gating techniques. Here, a comparative overview on voltage control of magnetism in all-solid-state and solid/liquid composites is presented within the context of the principal coupling mediators, i.e., strain, charge carrier doping, and ionic intercalation. Further, an exhaustive and critical discussion is carried out, concerning the suitability of using the common definition of coupling coefficient $\alpha_C = \frac{\Delta M}{\Delta E}$ to compare the strength of the interaction between electricity and magnetism among different magnetoelectric systems.

1. Introduction

Today's microelectronic and spintronic eras are witnessing an ever growing impulse toward the realization of novel nanoscale devices with enhanced functionalities as compared to their bulk counterparts. In the panorama of phenomena enabling the control of material properties at the nanoscale, the magnetoelectric (ME) effect, related to the coupling between magnetism and electricity in matter, holds a prominent role in world-wide research activities.[1–12] From a technological perspective, several low-power ME applications have been envisioned, comprising devices for memory storage and processing,[13,14] tuning and filtering of RF/microwave signals,[15,16] energy conversion and harvesting,[17,18] sensing,[19,20] and actuation.[21,22]

By definition, the direct ME effect is manifested when an electric polarization P is induced by usage of a magnetic field H in accordance with

$$\Delta P = \alpha_D \ \Delta H \tag{1}$$

where α_D defines the direct ME coupling coefficient. Alternatively, the converse ME effect is realized when a magnetization M arises from the application of an electric field E according to

$$\Delta M = \alpha_C \ \Delta E \tag{2}$$

where α_C denotes the converse[23] ME coupling coefficient. To date, a major stream of research focuses on the investigation of electric fields to control a variety of magnetic properties, including magnetic anisotropy,[24–32] magnetic transition temperature,[33–44] magnetic moment,[45–50] spin polarization,[51,52] exchange bias,[53–57] ferromagnetic resonance,[58–61] magnetic topology,[62,63] and magnetoresistance.[64–67]

Materials that exhibit inherent coupling between magnetic and electric degrees of freedom are classified into two broad categories,[1,68] the single-phase MEs and single-phase ME multiferroics (MFs). The former comprises those materials presenting intrinsic interactions between electric and magnetic polarizabilities. Cr_2O_3 is one of the first discovered and most investigated single-phase MEs,[69,70] concurrently displaying both antiferromagnetism and electric polarization. Under more stringent requirements, single-phase ME MFs manifest an intrinsic connection between ferromagnetic and ferroelectric orders, as for example, in the well-known $BiFeO_3$ (BFO)[71] and $TbMnO_3$.[72]

Since the strength of the ME effect is related to the values of electric and magnetic susceptibilities,[73] single-phase ME MFs feature larger values of magnetoelectric coupling coefficient α compared to single-phase MEs. For instance, in case of Cr_2O_3 the application of an electric field of 10^6 V cm^{-1} allows to flip only a few ferromagnetically coupled spins in a lattice containing around 10^6 antiferromagnetically coupled spins.[74] By contrast, full macroscopic reversal of the spins in a single-phase ME MF of $Dy_{0.7}Tb_{0.3}FeO_3$ was demonstrated upon application of a lower electric field of 50×10^3 V cm^{-1}.[47]

Dr. A. Molinari, Prof. H. Hahn, Dr. R. Kruk
Institute of Nanotechnology (INT)
Karlsruhe Institute of Technology (KIT)
Hermann-von-Helmholtz-Platz 1, 76344 Eggenstein-Leopoldshafen, Germany
E-mail: molinarialan86@gmail.com; robert.kruk@kit.edu
Prof. H. Hahn
KIT-TUD-Joint Research Laboratory Nanomaterials
Technical University Darmstadt
Jovanka-Bontschits-Strasse 2, 64287 Darmstadt, Germany
The ORCID identification number(s) for the author(s) of this article can be found under https://doi.org/10.1002/adma.201806662.

DOI: 10.1002/adma.201806662

Despite the promising results, there are a few factors hampering the research on single-phase ME MFs. For instance, it was found that, in nature, the conditions needed to concurrently promote ferroelectricity and ferromagnetism are generally unfavorable.[75] Furthermore, besides the dearth of single-phase ME MFs, often magnetic and electric ordering occurs at cryogenic temperatures with values of polarization and/or magnetization yet too small for practical applications.

A valuable workaround to circumvent the limitations associated with single-phase materials is offered by artificial ME composites. In these systems, the ME effect stems as a product property between their constituents, which, taken singularly, do not possess any inherent connection between electric and magnetic properties.[76] An intriguing advantage of artificial ME composites is the accessibility to a broad parameters space, including the combination of various materials, geometries, and coupling mediators.

Since the ME effect is of interfacial origin, a deep understanding of the phenomena that take place at interfaces—or propagate through them—is of crucial importance. The mechanisms acting as mediator of the ME coupling in artificial composites can be divided into three main groups (see **Figure 1**a). The first makes use of the stress induced by a piezoelectric actuator to modify the strain state of a magnetic material, and in turn also its magnetic response via magnetostriction. The second, which finds inspiration from the working principle of the field-effect transistor,[77] is based on the accumulation/depletion of charge carriers in a magnet by the polarization of a gate material. The third concerns the insertion/removal of ions into/from the lattice of a host magnet by using an ionic conductor, akin to the charging/discharging processes occurring in electrochemical batteries.

These coupling mediators operate at various length scales with respect to the spatial effects on the magnetic properties (see Figure 1b). Charge doping is a surface or near-surface effect, ionic migration can extend deeper into the bulk, whereas strain intervenes on a broader macroscopic scale. Under certain circumstances the ME effect may be the result of combination of multiple coupling mechanisms,[46,49,60,78] with the specific contributions not always straightforward to be identified. In particular, distinguishing between electrostatic and electrochemical effects is a hotly debated topic in the literature.[49,79–82]

In this respect, the physicochemical nature of the ME interface plays a key role in determining the response of a magnetic material upon application of an external electrical stimulus. Since the renaissance[83] of the studies on ME effect, the vast majority of research on artificial composites has focused on voltage-control of magnetism in all-solid-state ME systems. A typical configuration is represented by thin film heterostructures, where ME effect originates at the interface between two solid materials. Nevertheless, in the last few years, the landscape of ME systems has witnessed a growing interest stimulated by a parallel stream of research based on liquid-gating techniques. In this scenario, a magnetic material is put in contact with a liquid electrolyte solution. Differently from the strong chemical bonds formed at solid/solid interfaces, the main players promoting the ME effect are the mobile ions of the electrolyte, which can be accumulated onto (or pass through) the surface of a magnet by means of an external voltage (more details about this point are elaborated in the following sections).

Alan Molinari received his B.Sc. and M.Sc. degrees in physics from the University of Bologna and his Ph.D. degree in materials science from the Technical University of Darmstadt. Presently, he is a postdoctoral associate at the Institute of Nanotechnology (INT) of the Karlsruhe Institute of Technology (KIT). His research interests include the growth and characterization of complex oxide thin films and the investigation of the magnetoelectric effect in composite systems.

Horst Hahn is the Director of the Institute of Nanotechnology at Karlsruhe Institute of Technology. Previously, he held positions at Argonne National Laboratory, University of Illinois, Rutgers University and was full professor at TU Darmstadt from 1992 to 2004. His research interests include defects and diffusion in metals and ceramics, nanostructured and amorphous materials, tailored and tunable properties of nanostructures, energy materials, and printed electronics.

Robert Kruk was awarded his Ph.D. in solid state physics at the Jagiellonian University, Krakow, Poland. He works as a staff scientist at Institute of Nanotechnology (INT), Karlsruhe Institute of Technology. He is currently a leader of the "Electronically Tunable Materials" group at INT. His research interests include: reversible, electrochemical control of the physical (magnetic) properties in metals and oxide nanostructures; electrostatic doping via field-effect; reversible magnetic phase transitions induced with ionic liquid charging; spintronics; printed electronics; fabrication of solution-processed devices (transistors, etc.)

There are some nontrivial reasons explaining why solid/liquid ME composites developed later than all-solid-state approaches. From an experimental perspective, the usage of conventional aqueous electrolytes poses some restrictions in terms of the operating conditions. Concerning the applied voltage, water electrolysis already occurs at a low voltage of

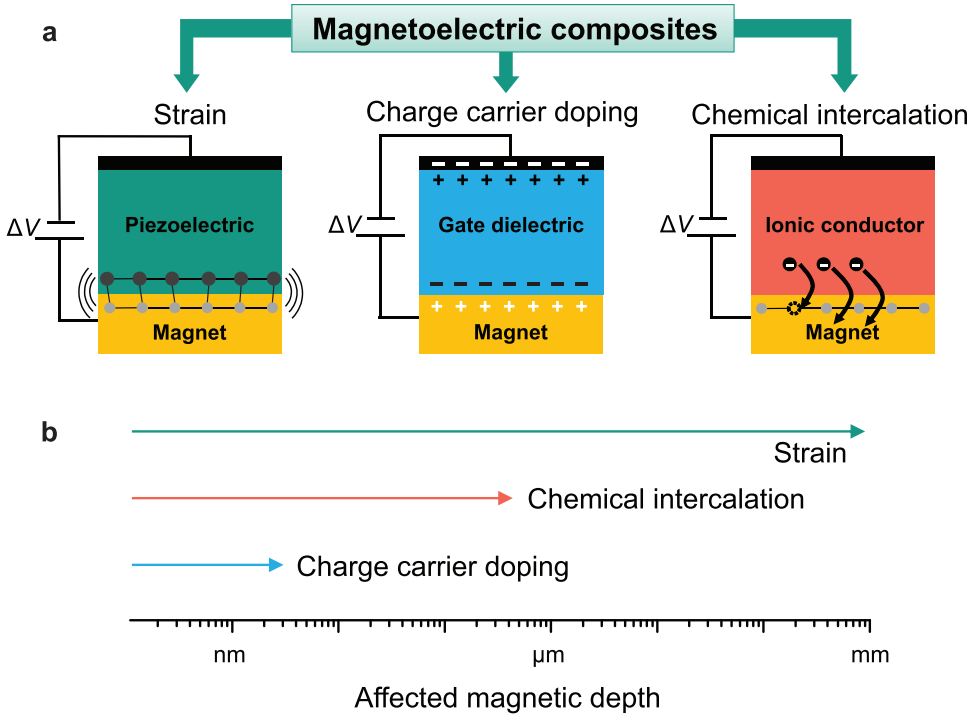

Figure 1. a) Mediators of the ME effect in ME composite systems. b) Typical affected length scales in a magnetic material via voltage-driven strain, charge carrier doping, and chemical intercalation. (b) Adapted with permission.[8] Copyright 2015, Wiley.

about 1.2 V and irreversible electrochemical reactions may occur at the electrode/electrolyte interface.[84] Besides, working operation is restricted close to room temperature, given the limited temperature window between freezing and boiling points. Further, certain electrolytes are toxic[85] or require careful handling due to the risk of flammability.[86]

Some of the above limitations are overcome by employing a special class of nonaqueous electrolytes, the so-called ionic liquids (ILs),[87] which behave as low melting point salts. ILs can withstand application of large voltages (up to about ±3.5 V) prior to decomposition and enable a broader temperature window in the liquid phase (typically 200 K < T < 600 K). Interestingly, ILs have also been effectively exploited in a frozen state to induce insulating to superconducting transitions in $SrTiO_3$ (STO)[88] and $KTaO_3$.[89] In addition, ILs display a low vapor pressure, implying a low risk of flammability and permitting to carry out experiments under vacuum conditions.

A general disadvantage of liquid electrolytes is the requirement of a suitable (and often cumbersome) housing to avoid spilling and degradation due to the interaction with the environment. Yet, this issue has been partially solved by implementation of ion gels,[90] consisting of semi-solid electrolyte solutions made of ILs embedded in a polymer matrix.

Despite the presence of some obstacles hampering the study of solid/liquid ME composites, they offer certain advantages when compared to all-solid-state MEs. For instance, concerning device fabrication, liquid gating methods permit to cover large surface area samples regardless of their morphology, such as thin films,[49] nanoparticles,[50] and porous materials,[91] by simply pouring the desired amount of electrolyte onto the specimen. On the contrary, the preparation of high-quality heterostructures with a low amount of structural defects, whose presence causes detrimental effects such as the formation of leakage current, can be very demanding in terms of optimization of the growth conditions and generally requires the use of costly deposition techniques, e.g., physical vapor deposition methods.[92] Furthermore, in certain circumstances, electrolyte gating has enabled stronger ME effects and significantly longer device lifetimes than those of all-solid-state MEs.

In the following sections, we analyze points of strength and criticalities of all-solid-state and solid/liquid ME composites in the light of the primary coupling mechanisms (strain, charge carrier doping, and ionic intercalation) acting at the interface, which enable the control of magnetism by application of electric fields.

2. ME Coupling via Strain

Strain-mediated ME effect is based on the idea of inducing magnetostriction in a magnetic material by making use of piezoelectricity.

A common configuration consists in the epitaxial growth of a magnetic thin film directly onto a single-crystalline piezoelectric substrate. By exploiting the structural phase transitions occurring in a $BaTiO_3$ (BTO) substrate as a function of different temperatures, Lee et al.[93] reported on a 70% modification of the magnetization in a 50 nm $La_{1-x}Sr_xMnO_3$ (LSMO) epitaxial thin film. Afterward, Eerenstein et al.[45] demonstrated the control of magnetization in similar LSMO/BTO epitaxial heterostructures using strain-controlled coupling induced by an external voltage. In this latter case, a giant modification of the magnetization up to 65% was reported using an electric

field of 5–10 kV cm^{-1}. The effect persisted even in case of an increase, removal, or reversal of the external voltage. The calculated α_C exceeded the best values achieved in bulk ME composites.[94] Similar studies were carried out on other composite oxide heterostructures of $Pb(Mg_{1/3}Nb_{2/3})_{0.72}Ti_{0.28}O_3$ (PMN-PT)/$La_{1-x}Ca_xMnO_3$ (LCMO),[78,95] PMN-PT/LSMO,[95] and Fe_3O_4/BTO.[96]

Besides fully oxide systems, there has been a great interest in combining ferromagnetic metal films,[24–26] alloys,[58–61,97–100] and multilayers[101–103] with piezoelectric materials. For instance, changes of the magnetic coercivity up to 40% were observed in Fe films deposited onto BTO substrates.[24] Tunability of the ferromagnetic resonance and bistable magnetization switching was shown to occur in FeGaB alloy films deposited onto lead zinc niobate-lead titanate (PZN-PT).[58] Reversible switching of magnetization from out-of-plane to in-plane was demonstrated in Cu/Ni multilayers grown onto BTO.[102]

One of the clearest examples of giant strain-mediated ME coupling was evidenced by the studies of Cherifi et al.[46] on FeRh/BTO heterostructures, where changes in magnetization of up to 550 emu cm^{-3} (with ≈70 emu cm^{-3} of reversible effect) were achieved close to room temperature by applying a voltage of about ±20 V (see **Figure 2**a). The presence of a butterfly-like response of the magnetization with respect to the applied voltage indicated that strain was the dominant driving force of the ME effect. Nonetheless, a slight asymmetry in the experimental data suggested also a small, but nonzero contribution of electrostatic charge doping at the film/substrate interface. The participation of both charge and strain comediated mechanisms in the control of ME effect has been investigated in other works[78,104,105] too. For instance, Nan et al.[105] demonstrated the coexistence of strain and charge effects in NiFe/PMN-PT composites, which displayed an enhanced ME coupling as compared to NiFe/Cu/PMN-PT systems, since the Cu buffer layer was responsible to suppress the contribution of interfacial charge doping.

Further insights into the intricate mechanisms of strain-coupling at the interface of magnetic films and piezoelectric substrates have been provided by a recent study on FeRh/PMN-PT composites,[99] which unveiled the presence of a time-dependent ME response (either transient or permanent) depending on the strength of the applied voltage.

In general, in order to have an effective strain coupling, a magnetic film has to be grown directly onto a macroscopic piezoelectric substrate rather than onto a piezoelectric film. In this way, substrate clamping effects are avoided which otherwise would hinder the propagation of strain through the heterostructure. Notably, an ingenious approach was proposed to overcome substrate clamping by fabrication of vertically aligned ME composite structures.[106–108] For example, electric-field driven reversal of magnetization was observed in ferromagnetic $CoFe_2O_4$ nanopillars embedded in a ferroelectric BFO matrix.[107] An alternative way to go beyond the limits imposed by the substrate constraint is to make use of flexible substrates. In this respect, strain-mediated ME coupling was investigated in BFO films deposited onto Ni tapes,[109] and in Ni films deposited onto compliant polymer substrates.[110]

Nonetheless, as a general remark, owing to the commonly needed bulk size of the piezoelectric element and the consequently required application of hundreds of volts for poling, strain-coupling in all-solid-state ME composites implies some limitations in terms of device miniaturization and energy efficiency.

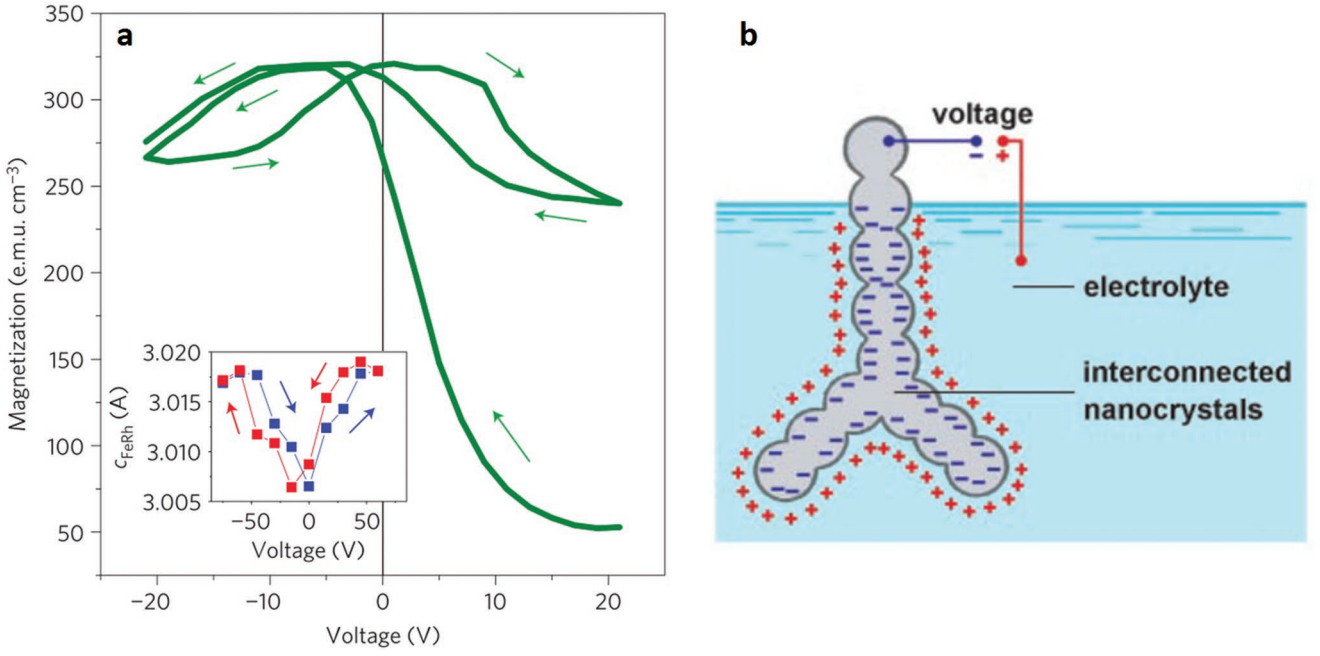

Figure 2. a) Control of the magnetization by voltage-driven strain in FeRh films grown onto BTO substrate. Reproduced with permission.[46] Copyright 2014, Springer Nature. b) Sketch of the principle of voltage-induced strain in solid/liquid ME composite systems. Reproduced with permission.[111] Copyright 2003, AAAS.

Apart from all-solid-state approach, a substantial strain can be obtained by utilizing liquid electrolytes. In 2003, Weissmüller et al.[111] discovered that charging with an electrolyte induces in porous Pt a strain change of about 0.15% (see sketch in Figure 2b), which is comparable to the magnitude achievable with commercially available piezoceramics. The origin of strain was attributed to the electrostatic pressure exerted by electric double layer charging (more details in the following section) within the interior of the crystallites. From an atomistic perspective, the change in strain is related to the modification of the electronic population due to band filling, which affects the equilibrium interatomic spacing. In this respect, strain is more effective in porous materials and powders compared to thin films, since the former are free to expand without being encumbered by the limitations arising from substrate clamping.

Concerning the field of ME coupling, about 1% tunability of the magnetic susceptibility in nanocrystalline Pd immersed in 1 M KOH aqueous electrolyte was demonstrated by applying less than 1 V.[112] Similar studies were also conducted on NiPd,[113] PdCo,[114] and AuFe[115] nanoporous alloys, all revealing a variation of magnetization not larger than a few percent.

3. ME Coupling via Charge Carrier Doping

Charge carrier doping via application of an electric field is probably the most widely investigated mechanism of ME coupling in composite systems.

Figure 3a,b shows a simplified scheme of the principle of electric field effect in all-solid-state and solid/liquid composite devices. In both cases, the basic structure is represented by a conventional capacitor, consisting of two conducting electrodes separated by a polarizable gate material. In order to study the ME effect, at least one of the two electrodes has to be a magnetic material (that is generally referred to as the working electrode), whereas the gate material can be either a polarizable solid (such as a dielectric or a ferroelectric) or an electrolyte. In both instances, the application of an external voltage ΔV between the electrodes induces the accumulation of charge carriers at the interface, a process known as electrostatic doping. The induction of electrons (or holes) in the magnet alters its electronic structure, hence affecting not only the electronic transport, but also the magnetic properties.[77,116]

However, there is a fundamental difference in the behavior of the electric field E: in all-solid-state devices E propagates through the entire thickness (typically 10 nm < d < 500 nm) of the dielectric (or ferroelectric), whereas in the case of electrolyte gating E is confined in the very proximity of the electrode surface. An immediate consequence is that, in solid/liquid composite devices, larger values of electric field ($E = \Delta V/d$ in first approximation) are typically achieved using lower voltages, thus resulting in lower energy consumptions. This is made possible by the very nature of electrolyte gating: upon application of an external voltage a thin layer of electrolyte counterions is electrostatically physisorbed onto the electrode surface and effectively screens the charge accumulated in the electrode within a short distance of ≈1 nm. Such interfacial charge configuration is denoted as electric double layer (EDL).[117]

Apart from electrostatic doping via EDL charging, the situation is somewhat more complicated in solid/liquid devices, since an additional mechanism of charge accumulation may be occurring. Depending on the electrode/electrolyte chemical compatibility, applied voltage, and working temperature, the strong interfacial electric field can promote the chemisorption (rather than the physisorption) of the electrolyte ions, with the subsequent onset of electrochemical redox reactions.[118–121] In this case, charge carriers are transferred across the electrode/electrolyte interface, implying the presence of a faradaic rather than an electrostatic process. The systems characterized by reversible charging/discharging processes via redox reactions are referred as pseudocapacitors.[118,119] Examples of electrode materials prone to pseudocapacitive behavior are VN,[122] MoO_2,[123] MoN,[124] MnO_2,[125–128] Fe_2O_3,[129,130] CoO_x,[131] NiO,[124] Nb_2O_5,[132] $LaMnO_3$,[133] and LSMO.[49] Notably, pseudocapacitors are of potential interest for investigation of ME effect, because several of them incorporate 3d transition metals, whose presence is a prerequisite for magnetism to occur.

Often, the lack of a clear distinction between electrostatic and electrochemical charging mechanisms is a source of ambiguity that calls for careful and systematic investigations.[49,79–82] In this

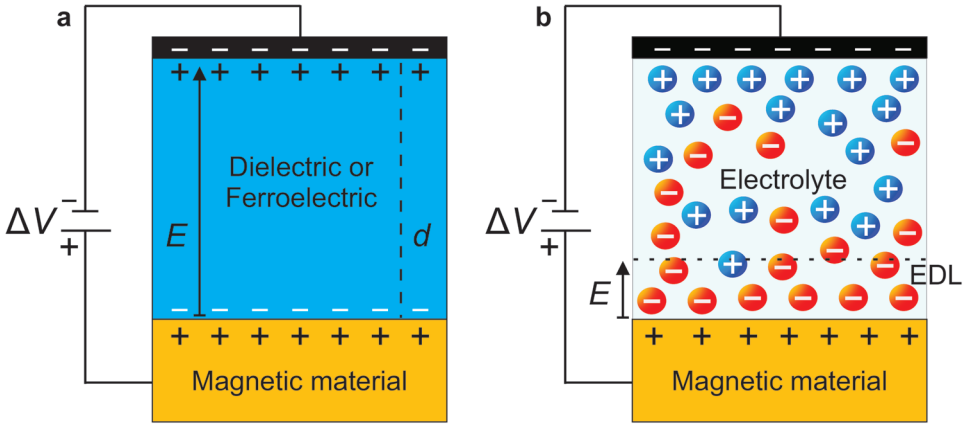

Figure 3. Principle of charge carrier doping in ME composites by gating with a) a polarizable solid or b) a liquid electrolyte. In the former case the electric field propagates through the entire thickness of the dielectric (or ferroelectric), whereas in the latter scenario the electric field is confined in proximity of the surface of the magnetic electrode. In both instances the charge carriers are accumulated at the interface.

regard, the analysis of the charging current–voltage (I/V) characteristics provides a precious tool to differentiate the main features of electrostatic and electrochemical charging. Specifically, a nearly rectangular-like shape of the I/V curves is expected for a capacitive behavior (electrostatic doping), whereas formation of more or less pronounced bumps should be present in the case of redox pseudocapacitance (electrochemical charge transfer).[49,120,121] Caution should be taken when the voltage is not swept quasi-continuously, but is kept fixed for a prolonged period of time (several minutes). Indeed, in a same ME system different response scenarios could be feasible when time-dependent mechanisms (e.g., ionic diffusion) become active.

Apart from the nature of the polarizable gate material, the electronic configuration of the magnet plays a key role in determining the response of the ME effect. If the magnet is in a metallic state, the applied E is screened by the high concentration of free charge carriers (e.g., $n \approx 10^{23}$ cm^{-3} in Fe) at the very proximity of the surface, since the Thomas–Fermi screening length is of the order of 1 Å. On the other hand, in case of magnetic semiconductors,[36] the lower charge carrier density (typically $n < 10^{20}$ cm^{-3}) allows the electric field to penetrate several nanometers into the material, thus affecting a bigger portion of the magnetic volume. Therefore, in order to optimize the ME effect, a careful adjustment of the surface-to-volume ratio of the devices is required.

Besides the electric field, another relevant parameter that determines the magnitude of ME effect is the surface charge density ΔQ that can be accumulated/depleted in the magnetic electrode (see **Table 1**). High-κ dielectrics as SiO_2, TiO_2, Al_2O_3, or HfO_2 can induce a surface charge of about 1–3 μC cm^{-2} (i.e., $\approx 10^{13} e^-$ cm^{-2}), ferroelectrics as BTO, $Pb(Zr_{1-x}Ti_x)O_3$ (PZT), or BFO can reach up to 30–80 μC cm^{-2} (i.e., $\approx 10^{14} e^-$ cm^{-2}), whereas electrolytes can overcome the former by exceeding values of 100 μC cm^{-2} (i.e., up to $\approx 10^{15} e^-$ cm^{-2}).

Table 1. List of dielectric constant κ, total variation of surface charge density ΔQ, and capacitance C of typical gate materials. The capacitance of solid dielectrics and ferroelectrics is estimated on the basis of the values of κ reported in the literature and assuming a dielectric thickness of 300 nm.

Gating type	Material	κ	ΔQ [μC cm^{-2}]	C [μF cm^{-2}]
Dielectric	SiO_2[211]	3.9	1–3	0.01
	Al_2O_3[137]	8–9	≈1	0.02
	HfO_2[212]	20–25	≈1	≈0.07
	ZrO_2[134]	22–25	1–10	≈0.07
	TiO_2[213]	50–80	1–2	≈0.2
	STO[65]	200–400	8–13	≈0.9
Ferroelectric	BTO[214]	≈3800	≈60	11
	PMN-PT[215]	≈3000	≈110	9
	PZT[216]	≈5000	≈140	15
	BFO[71]	30–300	≈140	≈0.9
Electrolyte	KOH/H_2O[217]	–	–	3–14
	$LiClO_4$/$C_4H_6O_3$[48]	–	22	27.5
	DEME-TFSI[49]	14.5	250	10–180
	EMIM-TFSI[80]	12	250	11
	$KClO_4$-PEO[218]	≈10	–	7.4
	TMPA-TFSI[185]	≈10	–	≈10

Since the induction of a surface charge implies the application of an external voltage, another commonly used figure of merit is the capacitance $C = \Delta Q/\Delta V$ (also expressed as $C = \varepsilon_0 \kappa \frac{S}{d}$ with $\varepsilon_0 = 8.85\ 10^{-12}$ F m^{-1} the permittivity of vacuum, κ the permittivity of the dielectric material, S the surface area of the capacitor, and d the thickness of the dielectric). In general, systems with large values of C are preferable, because they enable large accumulation of surface charge by using low voltages. Conventional EDL capacitors provide values of capacitance of about 5–20 μF cm^{-2},[117] whereas pseudocapacitors can reach 10–100 times larger values of C.[118,119]

After a brief description of the main mechanisms of charge carrier doping and associated parameters, we shall now present a survey of the results of charge-mediated ME coupling in all-solid-state and solid/liquid ME composites reported in the literature.

Early studies on electric field control of ferromagnetism were pioneered in 2000 by Ohno et al. in all-solid-state ME devices of magnetic semiconductors gated with solid dielectrics.[33] The group succeeded in switching from a ferromagnetic to a paramagnetic state a thin film (5 nm) of (In,Mn)As covered with a thick (800 nm) insulating polymide layer by applying an external voltage of ±125 V at 20 K. The estimated shift of T_C was around ±1 K. Subsequently, reversal of magnetization and a T_C shift of ±2 K were demonstrated in (In,Mn)As/SiO_2 composites by exploiting the change in magnetic coercivity induced by a surface charge modulation of 2.7×10^{12} cm^{-2}.[34] Following studies focused on (Ga,Mn)As thin films gated with dielectric ZrO_2[134] or ferroelectric P(VDF-TrFE).[135] The latter demonstrated an overall shift in T_C of ≈4 K together with nonvolatility of the ME effect. Afterward, nanodots of (Ga,Mn)As[136] and quantum dots of ($Mn_{0.05}Ge_{0.95}$),[137] respectively gated with HfO_2 and Al_2O_3 dielectrics, were studied as well. Despite the remarkable achievements, the main factor preventing the use of magnetic semiconductors in practical applications is the low temperature ferromagnetism (typically manifested below 100 K).

Differently from magnetic semiconductors, magnetic transition metals (e.g., Fe, Co, Ni) benefit from a higher Curie temperature, but feature a lower penetration depth of the electric field. Thus, ultrathin films (often below 1 nm) are generally chosen for electric field induced manipulation of magnetization. Maruyama et al.[138] reported on a magnetic anisotropy change of up to 40% in about four monolayers of Fe covered with a MgO (10 nm)/polymide (1500 nm) dielectric structure under the application of ±200 V. Chiba et al.[139] achieved a T_C shift of 12 K at room temperature in a 0.4 nm thick Co layer gated with a MgO (2 nm)/HfO_2 (50 nm) bilayer using a voltage of ±10 V. From a microscopic perspective, electric field control of magnetic domain wall motion was examined in ultrathin Co films charged with AlO_x[140] and HfO_2.[141] Magnetization reversal via electric field effect has been used to control the tunneling magnetoresistance in $Fe_{80}Co_{20}$ (0.7 nm)/MgO (1.5 nm)/Fe (10 nm) and in $Co_{40}Fe_{40}B_{20}$ (1.2 nm)/MgO (2 nm)/$Co_{40}Fe_{40}B_{20}$ (1.6 nm) trilayers.[142,143]

Another common choice for investigating the effect of an electric field on the magnetism is represented by the class of

magnetic and conducting oxides, such as LSMO, $SrRuO_3$ (SRO), $La_{1-x}Sr_xCoO_3$ (LSCO), or Sr_2FeMoO_6, which display charge carrier densities close to pure metals (10^{20} cm^{-3} < n < 10^{22} cm^{-3}). In addition, several of these complex oxides possess a similar crystal structure (i.e., perovskite) and lattice parameter of conventional dielectrics and ferroelectrics, e.g., STO, BTO, PZT, and BFO, hence facilitating the conditions for the growth of high quality epitaxial heterostructures with virtually defect-free interfaces.[92] Electric field effect has attracted particular attention in strongly correlated magnetic oxides, because in such systems the magnetic and transport properties are intrinsically correlated with each other. In a pioneering experiment of 1997, Mathews et al.[64] grew an epitaxial heterostructure of LCMO (30 nm)/PZT (300 nm) on top of a (001)-oriented $LaAlO_3$ single-crystalline substrate, with a configuration similar to that of a field effect transistor. By poling the ferroelectric with a voltage of ±7 V, a 300% modulation in LCMO resistance was attained. Afterward, magnetotransport measurements were carried out in several other manganite/dielectric composite heterostructures. Hong et al.[35,144] reported on a shift of 35 K and 50 K in the metal-to-insulator transition T_{MI} (reflecting an equal change in T_C) of LSMO/PZT devices. Interestingly, an electrically dead layer was found in LSMO films thinner than 3.7 nm, regardless of the polarization state of the PZT layer. The results on LSMO films with different thicknesses indicated an electric field screening length of the order of 0.2 nm. Afterward, Kanki et al.[145] tracked the magnetization and conductivity in a field effect $La_{0.85}Ba_{0.15}MnO_3$/PZT device, obtaining a shift of T_{MI} of only ≈1.5 K, but differently from previous works, this was realized at room temperature. In other studies, STO was utilized as gate dielectric in combination with thin films of LSMO. Pallecchi et al.[65] observed a maximum shift in T_{MI} of 43 K and a resistivity modulation of up to 250% in 7 unit cells LSMO films. On the other hand, thinner LSMO films were insulating and almost insensitive to field effect modulation. Brivio et al.[37] put to test the effect of back-gated (Ag/LSMO/STO/STO:Nb substrate) and top-gated (Au/STO/LSMO/STO substrate) geometries. Upon charge carrier doping, the former configuration did not produce any measurable variation in T_C, whereas in the latter case a shift of 5 K was found at room temperature. The reason for the different responses was ascribed to the presence of an electric dead layer at the LSMO/STO interface in the back-gated setup. Additional studies conducted on LSMO/PZT heterostructures via quantitative techniques, such as superconducting quantum interference device magnetometry and (calibrated) magneto-optical Kerr effect, revealed variations in both the critical temperature (of up to 20 K) and magnetization of LSMO, after PZT poling.[38,39,41] For instance, as evidenced by Leufke et al.,[41] the nearly perfect superposition of the ferroelectric and ferromagnetic hysteresis loops (see **Figure 4**a) provided strong evidence that charge carrier doping rather than strain was the dominant mechanism of ME coupling. Lu et al.[146] found that thicker LSMO films, in the range of 10–50 nm, gated with BTO did not manifest any significant shift in T_C. In addition, the authors estimated a maximum relative variation of LSMO magnetization of about 27% for the thinnest (10 nm) LSMO sample, and, in contrast with previous reports,[144] a penetration depth of the electric field of up to 3 nm. The latter value corresponded to the expected LSMO thickness to completely

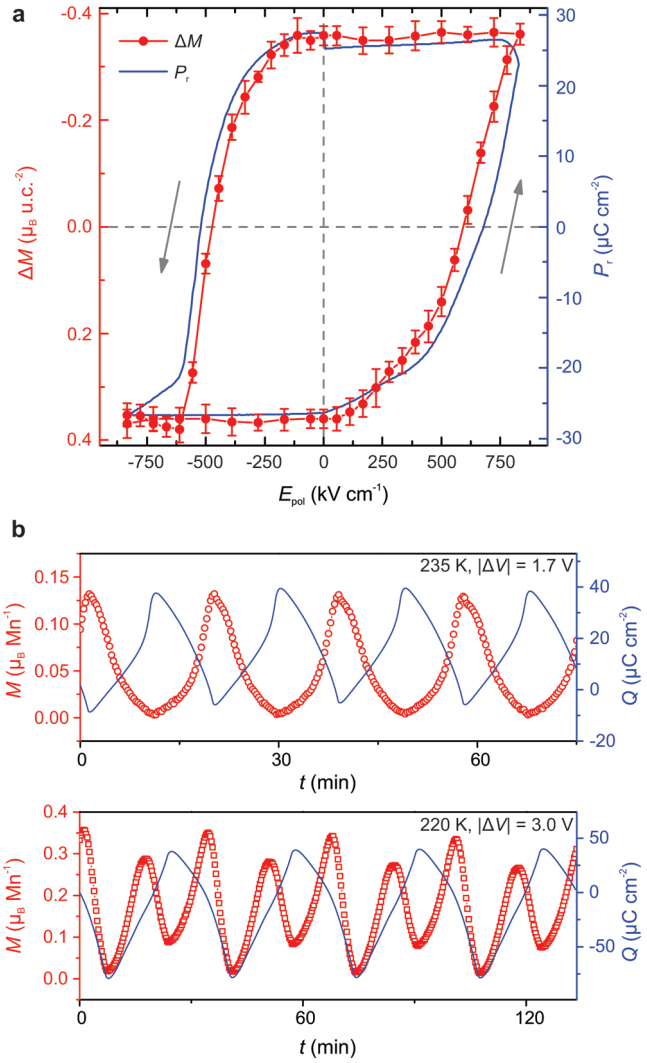

Figure 4. a) Comparison of ferromagnetic and ferroelectric hysteresis loops in LSMO/PZT heterostructure films. Reproduced with permission.[41] Copyright 2013, American Physical Society. b) Reversible on–off switching of magnetism in LSMO films upon surface charge modulation via ionic liquid gating. Reproduced with permission.[42] Copyright 2018, Wiley.

suppress the magnetization considering the total interfacial charge accumulated by poling the BTO ferroelectric.

The intriguing characteristics of fully oxide heterostructures fostered the analyses of several other materials combinations, such as LCMO/BFO,[147] SRO/STO,[52] SRO/BTO,[148] Fe_3O_4/BTO,[149] $CaMnO_3$/$CaRuO_3$,[150] and LSMO/PZT.[151,152]

The investigation of charge carrier doping in solid/liquid ME composites started in 2007, at a later stage than the seminal studies on all-solid-state ME composites, when Weisheit et al.[30] demonstrated a change of 4.5% in the magnetic coercivity of FePt ultrathin films (≈2 nm) immersed in a non-aqueous electrolyte, at room temperature, with application of just 0.6 V. Thereafter, other ferromagnetic metals and alloys, magnetic semiconductors, and magnetic oxides were analyzed via electrolyte gating.

Concerning magnetic metals, Shimamura et al.[40] examined ultrathin films (0.4 nm) of Co capped with a protective

MgO layer (2 nm) and gated with 1-ethyl-3-methylimidazolium bis(trifluoromethylsulfonyl)imide (EMI-TFSI) IL. A large shift in T_C of about 100 K was observed upon application of ±2 V for 30–60 min and attributed to EDL charging. A more recent work on ultrathin Co films gated with diethylmethyl(2-methoxyethyl)ammonium bis(trifluoromethylsulfonyl)imide (DEME-TFSI) IL revealed the presence of different charging regimes depending on the applied voltage.[153] Reversible electrostatic doping leading to a shift of up to 219 Oe in the ferromagnetic resonance field was seen for $-1.5 < V < 1.5$, whereas larger voltages triggered irreversible electrochemical reactions at the interface, accompanied by decomposition of the Co electrode. With respect to magnetic alloys, electrolyte gating was used as a viable means to substantially reduce the magnetic coercivity of CuNi[32] and FeCu[154] porous films.

In case of magnetic semiconductors, Yamada et al.[36] managed to trigger a transition from a low-carrier paramagnetic state to a high-carrier ferromagnetic state in $(Ti,Co)O_2$ films using two kinds of electrolytes (DEME-TFSI IL and $CsClO_4$ dissolved in polyethylene oxide (PEO)). Besides, a 14 K shift in T_C was attained in magnetic semiconductor films of (Ga,Mn)As gated with a polymer electrolyte ($KClO_4$ in PEO) by applying a voltage ranging from −1 to 3 V, although irreversible effects were observed beyond 2 V.[155]

A large portion of the research on solid/liquid MEs pertains the gating of magnetic oxides, which often exhibit a robust resistance against the possible occurrence of irreversible electrochemical reactions. In 2013, Mishra et al.[48] reversibly tuned the magnetization up to 2.5% of a LSMO nanopowder immersed in a liquid electrolyte by an electrostatic surface charge modulation of 22 μC cm^{-2}, using a potential window of less than 1 V at room temperature. Subsequently, quantitative studies of ME coupling in epitaxial films of LSMO gated with DEME-TFSI IL revealed that the interfacial charging processes progressively move from electrostatic doping to surface redox pseudocapacitance upon increasing the external voltage.[49] In case of 13 nm films, the attained large values of surface charge up to 250 μC cm^{-2} enabled a maximum reversible modulation in magnetization of about 30% at room temperature. By optimizing the surface to volume ratio of the devices, repeated suppression and recovery of ferromagnetism, with a T_C shift of about 26 K, was demonstrated in ultrathin LSMO films (≈3 nm).[42] In addition, the magnetic response was flexibly modulated in-phase or antiphase with respect to the induced surface charge by judiciously adjusting the applied bias voltage (see Figure 4b). Several other comprehensive studies contributed to disentangle the complex relationship between charge carrier doping and magnetism in electrolyte-gated magnetic oxides, including investigations on LCMO,[80,91] LSMO,[43,156] $LaMnO_3$,[67] $Pr_{1-x}(Ca_{1-y}Sr_y)_xMnO_3$,[157,158] LSCO,[82] Fe_3O_4,[159] and γ-Fe_2O_3.[160]

4. ME Coupling via Ionic Intercalation

If electrostatic and electrochemical charge doping mechanisms are primarily surface effects, voltage-driven chemical intercalation of ionic species opens a new pathway to the control of magnetism in bulk materials. Recently, the field of magnetoionics has generated a flurry of research activities, based on the idea of mimicking the working principles of electrochemical batteries or fuel cells.

GdO_x, a rare earth oxide with a large mobility of oxygen ions, has been exploited as a solid state oxygen reservoir in combination with magnetic metals.[28,161–163] By applying an external voltage, the oxidation front at the interface of Co/GdO_x heterostructures[28] could be moved back and forth, which in turn allowed to toggle the easy axis of the magnetization direction from out-of-plane to in-plane in a few monolayers of Co (see **Figure 5**a). At room temperature, the switching process required application of 5–10 V for several minutes. However, it was proven that usage of a higher temperature of about 100 °C or local laser-heating strongly enhanced the O^{2-} diffusion, which enabled a dramatic reduction in the ME response time down to hundreds of microseconds. Afterward, Gilbert et al.[162] demonstrated a semi-reversible control of bulk magnetization in thicker Co films (15 nm) via voltage-driven O^{2-} diffusion from a GdO_x film.

Apart from oxygen ions, an alternative carrier used in solid-state magnetoionics is represented by Li^+ cations.[164,165] In this respect, Zhu et al.[164] reported on ≈100% magnetization modulation of magnetic domains and reversible domain wall motion over a distance of ≈100 nm in SRO/$LiFe_5O_8$ layers, by controlling the deintercalation/intercalation of Li^+ ions.

If the majority of studies on ME effect via strain and charge doping mechanisms focus on all-solid-state devices, owing

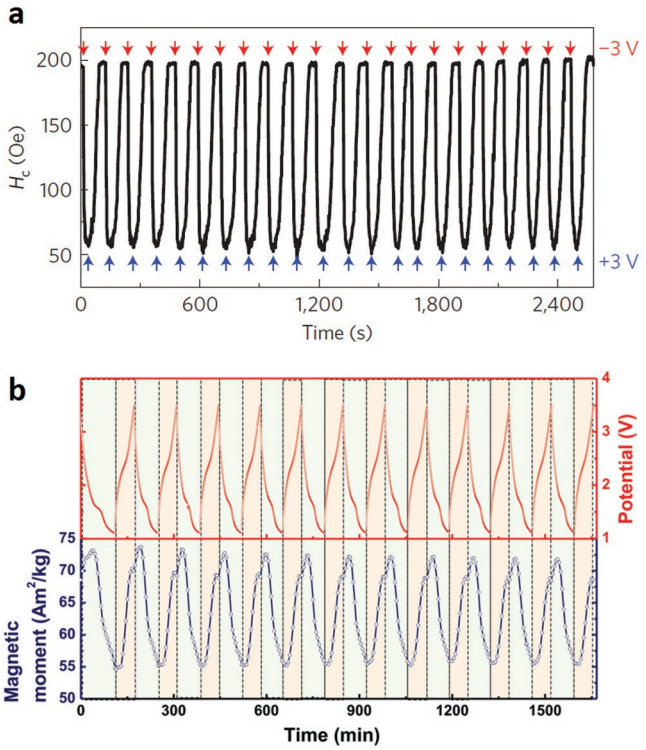

Figure 5. a) Modulation of the magnetic coercivity via voltage-controlled oxygen ions diffusion in Co/GdO_x heterostructures. Reproduced with permission.[28] Copyright 2015, Springer Nature. b) Reversible control of the magnetization upon voltage-driven migration of lithium ions in γ-Fe_2O_3 powder immersed in Li-based electrolyte. Reproduced with permission.[50] Copyright 2014, Wiley.

to the widespread success of electrochemical lithium batteries, a vast portion of the research on magnetoionics is covered by solid/liquid composites. One of the first examples of insertion/removal of Li^+ ions into/out of the lattice of a host magnet was shown by Dasgupta et al.,[50] who succeeded in obtaining a reversible magnetic modulation of ≈30% at room temperature in a lithiated/delithiated γ-Fe_2O_3 powder (see Figure 5b). This compound was selected because its crystal structure (inverse spinel) contains several vacancy sites, whose presence facilitates the migration of Li^+. Furthermore, the applied voltage was carefully chosen within a specific potential window in order to insert/remove the cations without disrupting the crystal structure of the electrode. This novel and effective approach permitted a high cycling stability upon charging/discharging the devices several times. Thereafter, following a similar approach, a larger variation of magnetization up to 50% and 70% was obtained in bulk $CuFe_2O_4$ and $ZnFe_2O_4$ powders,[44] respectively. An ample literature concerning the control of magnetism via lithiation is now available, including the studies on α-$LiFe_5O_8$,[166] α-Fe_2O_3,[31] Fe_3O_4,[167] $CoFe_2O_4$,[21] $Co_{0.5}Ni_{0.5}Fe_2O_4$,[21] $NiFe_2O_4$,[21] $MnFe_2O_4$,[168] $LiNi_xMn_yCo_zO_2$,[169,170] and donor/acceptor metal–organic frameworks.[171]

Besides lithium migration, oxygen diffusion has also been used to control the magnetic properties in the near-surface regions and in the bulk of magnetic materials in contact with liquid electrolytes. A magnetization change of up to 64% and 86% was respectively attained in thin films[172] and nanoislands[173] of iron covered with 1 M KOH aqueous solution via quasi-reversible electrooxidation and electroreduction processes. A similar approach was also exploited to manipulate the magnetization and coercivity of electrolyte-gated FePt[174] and CoPt[175] alloys.

Regarding magnetic oxides, investigations on LSMO/IL devices[176,177] pointed out the formation and annihilation of oxygen vacancies affecting deep portions (down to 20 nm) of the magnetic film when large voltages were applied for prolonged periods of time, which caused a substantial variation of the metal-to-insulator transition temperature. Similar results were also attained in ion gel gated LSCO films,[178] where depth profile measurements revealed that the oxygen vacancies were present through the entire film thickness (≈40 unit cells). Further, a shift in the onset of magnetoresistance of up to 30 K was induced by O^{2-} migration in SRO films gated with EMI-TFSA ion gel.[179] Notably, this work underlined also a strong dependence of the mechanism of oxygen diffusion as a function of the applied voltage ramp rate. Electrolyte-gated Co_3O_4 films featuring room-temperature paramagnetism displayed the emergence of a ferromagnetic state due to creation of Co clusters upon diffusion of oxygen ions.[180]

So far, investigations on magnetoionics have been focused on the voltage-control of single ionic species. Nonetheless, a recent work by Lu et al.[181] opened the way to greatly enrich the functionality of materials by electric-field control of multistate phase transformations. It was proven that IL-gated epitaxial thin films of $SrCoO_{2.5}$ (an antiferromagnetic insulator) can be transformed into $SrCoO_{3-\delta}$ (a ferromagnetic metal) upon oxidation and $HSrCoO_{2.5}$ (a weakly ferromagnetic insulator) upon hydrogenation.

5. Other Forms of ME Coupling

The spectrum of phenomena encompassing the electric-field control of magnetism is not restricted to the conventional mechanisms of strain, charge carrier doping, and ionic intercalation discussed above. Here, we mention some other relevant approaches to realize the ME effect.

When a magnetic material is put in contact with either a single-phase ME or a single-phase ME MF, the electric field control of magnetism can be accomplished via interfacial exchange coupling.[53,56,66] Such ME phenomenon, which has sparked intensive research in the area of spintronics, has been widely discussed in comprehensive review articles.[8,9,13] A prototypical system[66] featuring the mechanism of exchange coupling is represented by ferromagnetic $Co_{0.9}Fe_{0.1}$ grown in contact with BFO (a ferroelectric antiferromagnet with weak ferromagnetism due to spin canting): upon the application of an electric field, the canted moment of BFO can be reversed and this, in turn, permits to switch the magnetization direction of $Co_{0.9}Fe_{0.1}$.

A peculiar form of charge-mediated ME effect was proposed by combining solid/liquid polarizable gate materials.[182–186] Such hybrid gate configuration was utilized to reversibly control the interfacial magnetism in LSMO/PZT heterostructures by means of IL-assisted polarization switching.[186]

Conventionally, ME effect implies the modification of the magnetic properties starting from a robust ferromagnetic material. Nonetheless, studies have been reported on the emergence of ferromagnetism stemming from a decrease in the electron concentration at the $LaAlO_3$/STO interface, both materials known for being nonmagnetic oxides.[187]

Another largely unexplored area of research is represented by ME interactions in ferroelectric and ferromagnetic liquid crystals.[188–190] They are composed of molecules with a high degree of shape anisotropy, whose orientational state can be readily manipulated by external stimuli, such as electric and magnetic fields, and light irradiation.

Recently, electric field effect was exploited to write and erase magnetic skyrmions.[62,63] This new degree of freedom, related to the control of complex magnetic topologies via application of electric fields, may be potentially implemented for developing novel racetrack memories.[191,192]

6. Comparison of Technologically Relevant ME Characteristics

After a general presentation on the broad landscape of ME phenomena and systems, we shall now critically discuss some of the most relevant parameters in the perspective of potential ME applications.

For long time, a major effort of the scientific community was to find the best strategies in order to enhance the magnitude of the ME effect. Conventionally, the converse ME coupling coefficient, $\alpha_C = \frac{\Delta M}{\Delta E}$ (see Equation (2)), expressed in units of [s m^{-1}] or [Oe cm V^{-1}], is used as benchmark to evaluate the strength of the ME coupling. Despite its rationale and beauty, several examples in the literature reveal that a strict use of such definition can be quite challenging.

A mean ME coupling coefficient $\alpha_C = \frac{\Delta H}{\Delta E} \approx 0.1$ Oe cm V^{-1} was estimated by Lou et al.[59] in FeGaB/PZN-PT heterostructures, which considers ΔH, related to a shift in the resonance frequency of the magnetic field, rather than a change in magnetization ΔM. Heron et al.[66] introduced $\alpha_C = \frac{2\mu_0 M_s t}{R_{AP} - R_P} \frac{dR(V)}{dV}$, which includes the change in resistance in exchange-coupled $Co_{0.9}Fe_{0.1}$/Cu/$Co_{0.9}Fe_{0.1}$/BFO spin valve heterostructures. Studies of charge-mediated ME effect in LSMO/PZT[41] and LSMO/IL[49] composites adopted $\alpha_C = \frac{\Delta M}{\Delta Q}$, since precise values of the surface charge density induced at the interface were properly quantified. For the microscopic analysis of the ME effect in multiferroic clusters,[193] $\alpha = \frac{2P_s m}{K_{BFC}}$ was defined, where K_{BFC} serves as calibration factor between the signals measured locally via piezoresponse and magnetic force microscopies. Recently, some studies of ME effect in solid/liquid composites[42,153,159] employed $\alpha_C = \frac{\Delta M}{\Delta V}$, which directly correlates the change of magnetization to the applied voltage rather than the electric field.

Thus, the question arises whether or not the use of $\alpha_C = \frac{\Delta M}{\Delta E}$ allows for an adequate comparison of the strength of the ME effect among systems that are characterized by different coupling mediators and physical quantities.

Formally, a rigorous usage of Equation (2) requires a precise determination of both magnetization M and electric field E. Concerning the former, it is worth to notice that, in several reports, it is not M to be affected by an applied E, but rather a magnetic field H. The latter may relate to a coercive field H_c,[24,26,194] an exchange bias field H_{EB},[56,195] or a ferromagnetic resonant field H_r.[59,61] Therefore, in order to avoid ambiguity, it should be specified which physical quantity (ΔM or ΔH) is being considered in the definition of α_C.

Further, the determination of an apparently standard physical quantity as the electric field E may conceal some unexpected pitfalls. As previously mentioned, generally, the electric field is calculated according to the relation $E = V/d$, by considering a parallel-plate capacitor configuration with a uniform distribution of the lines of E. This approximation is broadly accepted when the surface area of a ME device is much larger than its thickness. Nevertheless, it should be kept in mind that in the case of nanoscale-based devices, this assumption calls for atomically flat, sharp interfaces over large areas. Furthermore, this criterion does not hold any longer when local probe techniques, as scanning probe microscopies, are used, due to the nonuniformity of the E-field produced underneath the tip.

Another factor to consider is the eventuality of a nonuniform distribution of the electric field within a magnetic material. Indeed, if a material presents intrinsic inhomogeneities[196,197] or undergoes metal to insulator phase transitions (e.g., both conditions occurring in strongly correlated manganites), the effective penetration depth of E may substantially vary in different areas of the specimen, and thus it is difficult to be computed.

Aside from the potential issues in accurately determining the values of E, the situation becomes even more entangled when the aim is to compare the ME effect realized via different coupling mediators.

It is interesting to critically compare the values of $\alpha_C = \frac{\Delta M}{\Delta E}$ for two examples of state-of-the-art ME composites based on strain[46] and charge[38] coupling.

The first refers to ferromagnetic FeRh films grown onto piezoelectric BTO substrates. By poling the device with a voltage of 21 V, which corresponds to $E = 0.4$ kV cm^{-1} (given a substrate thickness $d = 0.5$ mm), a reversible variation of magnetization $\Delta M \approx 70$ emu cm^{-3} was achieved in FeRh, thus resulting to a value of $\alpha_C \approx 1$ Oe cm V^{-1}. The second pertains ferromagnetic/ferroelectric bilayers of LSMO/PZT deposited onto STO substrate. By applying ±10 V, which corresponds to $E = \pm 400$ kV cm^{-1} (given a PZT thickness $d = 250$ nm), the switching from hole accumulation/depletion states induces a change of magnetization $\Delta M \approx 22$ emu cm^{-3} (≈0.14 μ_B Mn^{-1}) in LSMO, which corresponds to $\alpha_C \approx 0.8 \times 10^{-3}$ Oe cm V^{-1}.

Apparently, the larger α_C in the first instance shall be simply attributed to the long-range nature of the strain effect, which affects bigger portions of the magnetic active volume than in case of interfacial electrostatic charge doping. Nonetheless, comparing the parameters of the two scenarios, ΔM and ΔV are nearly commensurate, whereas there is a marked difference of three orders of magnitude in the electric field E. Consequently, the latter is the main factor resulting in the very different values of α_C.

The impact of E on the calculation of α_C is even more dramatic when considering charge-mediated ME effect in solid/liquid ME composites. Recently, in IL-gated LSMO films,[42] a $\Delta M \approx 54$ emu cm^{-3} was attained by using a potential window $\Delta V \approx 3$ V, which, owing to the intrinsic small thickness ($d \approx 1$ nm) of EDL capacitors, corresponds to an ultrahigh interfacial electric field $E \approx 30$ MV cm^{-1}. Therefore, albeit the variation in magnetization is comparable with the previous examples of all-solid-state MEs, and it is obtained by application of a lower voltage, according to Equation (2), the apparent strength of the ME effect is much smaller. This paradoxical situation strongly suggests that a more appropriate definition of α_C should be introduced in order to compare ME coupling among different ME systems.

Hence, since the presence of an electric field E requires the application of a defined voltage V, an alternative, more general figure of merit could be represented by the ME-voltage coefficient

$$\alpha_{C,V} = \frac{\Delta M}{\Delta V} \tag{3}$$

for a change in magnetization, or similarly, for a change in magnetic field

$$\alpha_{C,V} = \frac{\Delta H}{\Delta V} \tag{4}$$

Values of ME-voltage coefficients for differently coupled ME systems and other relevant parameters, including degree of reversibility, cycling time, and working temperature, are summarized in **Tables 2** and **3**.

On the whole, solid/liquid ME composites present similar (if not larger) variations of ΔM and ΔH as well as a lower price in terms of the applied voltage when compared to their

Table 2. List of parameters of interest in various ME systems, including kind of coupling mechanism, variation in magnetization ΔM, applied voltage ΔV, calculated ME voltage coefficient $\alpha_{C,V}$, presence of reversibility, cycling time, and working temperature. The magnetic conversion factor for the calculation of $\alpha_{C,V}$ is 1 emu $cm^{-3} = 4\ \pi$ Oe. The abbreviations refer as following: room temperature (RT), ethylene carbonate (EC), diethyl carbonate (DC), ethyl acetate (EA), propylene carbonate (PC).

System	Materials	Coupling	ΔM [emu cm^{-3}]	ΔV [V]	$\alpha_{C,V}$ [Oe V^{-1}]	Reversible	Cycling time [s]	T [K]	Ref.
All-solid-state	$CoFe_2O_4$/BFO	Strain	20	10	25	–	–	RT	[107]
	LSMO/BTO	Strain	71	200	4.5	No	–	199	[45]
	FeRh/BTO	Strain	70	21	42	Yes	–	385	[46]
	FeRh/BTO	Strain	550	21	329	–	–	350–400	[46]
	LSMO/PMN-PT	Strain	19	400	0.6	Yes	–	330	[95]
	LCMO/PMN-PT	Strain	12.5	400	0.4	Yes	–	210	[95]
	LCMO/PMN-PT	Strain	24	480	0.6	Yes	–	10	[78]
	$Dy_{0.7}Tb_{0.3}FeO_3$	Exchange striction	58	350	2	Yes	1.5	2.5	[47]
	LSMO/PZT	Charge	32	20	14	Yes	–	100	[38]
	LSMO/PZT	Charge	120	20	75	–	–	100	[151]
	$LiCoO_2$/LISICON/Fe_3O_4	Ionic	40	4	125	Yes	8×10^4	RT	[165]
Solid/liquid	$Pd_{90}Co_{10}$/$LiClO_4$ in EA	Strain	0.16	2	1	Yes	10^4	RT	[114]
	LSMO/$LiClO_4$ in PC	Charge	1.3	0.8	20	Yes	7500	RT	[48]
	LSMO/DEME-TFSI	Charge	54	3	226	Yes	10	220	[42]
	Fe_3O_4/$LiPF_6$ in DC + EC	Ionic	2.3	0.5	58	Yes	–	RT	[167]
	γ-Fe_2O_3/$LiPF_6$ in EC + DC	Ionic	90	2.4	470	Yes	10^3	RT	[50]
	α-Fe_2O_3/$LiPF_6$ in PC	Ionic	530	1.5	4400	Yes	–	RT	[31]
	$ZnFe_2O_4$/$LiPF_6$ in EC + DC	Ionic	66	2.25	370	Yes	–	RT	[44]
	$CuFe_2O_4$/$LiPF_6$ in EC + DC	Ionic	85	2	530	Yes	–	RT	[44]
	$MnFe_2O_4$/LBC3015B	Ionic	10	1.5	84	Yes	8×10^3	RT	[168]
	$SrCoO_{3-\delta}$/IL	Ionic	346	4	1100	Yes	≈2000	10	[181]

Table 3. List of parameters of interest in various ME systems, including kind of coupling mechanism, kind of affected magnetic field, variation in magnetic field ΔH, applied voltage ΔV, calculated ME voltage coefficient $\alpha_{C,V}$, presence of reversibility, cycling time, and working temperature. The abbreviations refer as following: ferromagnetic resonance field (H_r), coercive field (H_c), exchange bias field (H_{EB}), room temperature (RT), propylene carbonate (PC).

System	Materials	Coupling	Kind of H shift	ΔH [Oe]	ΔV [V]	$\alpha_{C,V}$ [Oe V^{-1}]	Reversible	Cycling time [s]	T [K]	Ref.
All-solid-state	FeGaB/PZN-PT	Strain	H_r	750	400	1.8	Yes	10^{-9}	–	[59]
	FeGaB/PZN-PT	Strain	H_r	473	10	47	Yes	10^{-9}	–	[59]
	FeGaB/PZN-PT	Strain	H_r	500	7.5	67	Yes	10^{-10}	–	[58]
	Fe/BTO	Strain	H_c	27	1000	0.027	–	–	250	[37]
	Fe/BTO	Strain	H_c	10	2000	0.005	Yes	–	150	[25]
	Co/PVDF-TrFE	Charge	H_c	25	24	1	–	–	–	[27]
	Co/GdO	Ionic	H_c	140	6	23	Yes	10^{-6}–500	300–400	[28]
	Co/GdO	Ionic	H_c	200	12	17	Yes	500	–	[219]
	SiO_2/MgO/CoFeB	Charge	H_c	70	100	0.7	Yes	–	12	[29]
	CoFeB/IrMn/PMN-PT	Strain	H_{EB}	30	400	0.075	Yes	–	RT	[54]
	LSMO/BFO	Charge	H_{EB}	125	120	1	Yes	–	5.5	[56]
	FeNi/$YMnO_3$	Exchange	H_{EB}	60	1.2	50	–	–	2	[195]
	FePt/Na in PC	Charge	H_c	45	0.6	75	Yes	–	RT	[30]
Solid/liquid	α-Fe_2O_3/$LiPF_6$ in PC	Ionic	H_c	60	1.5	40	Yes	–	RT	[31]
	CuNi/Na in PC	Charge	H_c	31	14	2.2	–	–	RT	[32]
	Co/DEME-TFSI	Charge	H_r	90	2.5	36	Yes	600	RT	[153]
	Fe_3O_4/DEME-TFSI	Charge	H_r	750	3	250	Yes	300	100–300	[159]

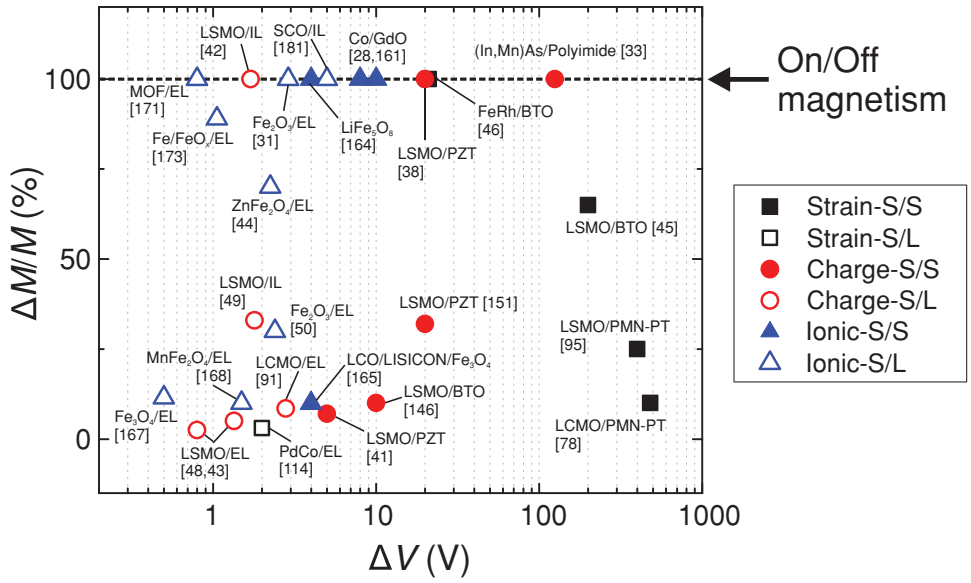

Figure 6. Comparison of the relative variation in magnetization as a function of the applied voltage in case of different ME composite systems (S/S = all-solid-state, S/L = solid/liquid) and ME coupling mediators (strain, charge carrier doping, and ionic migration).

all-solid-state counterparts. Therefore, larger values of ME coupling coefficient $\alpha_{C,V}$ are typically obtained via electrolyte gating techniques. To date, the largest changes in ΔM are reached by means of strain coupling in all-solid-state MEs,[46] whereas chemical intercalation is the most effective tool in solid/liquid MEs.[31] The most pronounced variation in ΔH regards the shift in ferromagnetic resonant field via strain effect in all-solid-state[59] composites and via charge carrier doping in solid/liquid[159] composites.

Concerning the relative variation of magnetization $\Delta M/M$ (see **Figure 6**), on/off switching of magnetism is already established in various ME composite systems. However, independently of the kind of coupling mechanism, one to two orders of magnitude lower values of voltage are required in solid/liquid ME devices. Concerning all-solid-state ME devices, the application of lower voltages is needed when the kind of coupling mediator moves from strain, to charge doping or ionic intercalation.

Besides a robust ME effect and a low-voltage application, other important prerequisites in the perspective of future technological applications are represented by the device endurance and the switching time, which often do not receive a deserved attention.

Regardless of the specific technical functionalities that are envisioned, magnetism should be manipulated at will as many times as possible. Thus, a careful analysis of the level of reversibility of the ME effect and of the reasons for its eventual loss is of primary importance. In particular, application of high voltages, as often occurs in strain-mediated solid-state MEs, poses a risk of catastrophic failure already after a few cycles due to sparking, contact loosening, and aging effects in relation to defect orientation.[24,45] The nature of the interface is another factor that can negatively impact on the cycling stability. Indeed, when ME effect is realized at a metal/oxide interface, the reactive surface of metals and alloys may undergo irreversible oxidation processes, triggered by the simple contact with an oxide material and further promoted via application of an external voltage.[24,66,198] The potential issue of materials compatibility can be limited, to a great extent, when the interface is composed of only oxides. Despite the usage of lower voltages, the presence of a strong interfacial electric field in solid/liquid devices makes them potentially vulnerable to irreversible electrochemical reactions. The durability associated with electrolyte gating techniques strongly depends on the kind of charging/discharging mechanism being involved. Electrostatic charge doping allows EDL capacitors to have a lifespan beyond 10^6 cycles, pseudocapacitors, based on surface or near-surface redox reactions, can withstand 10^4–10^6 cycles of working operation, whereas electrochemical batteries, relying on bulk ionic migration, can only reach a few thousand cycles.[118,199]

The speed of the ME response is another critical parameter to be taken into account, especially for the potential realization of ME memories and ME antennas. Strain and charge-mediated solid-state devices, relying on polarization switching by means of short voltage pulses, provide the fastest response time down to the nanosecond range.[143,200,201] By contrast, ionic intercalation through bulk magnetoionics is a rather slow process, which typically requires hundreds of seconds, unless operated at high temperatures or via laser-assisted heating.[28]

On all the fronts of ME coupling, solid/liquid devices display markedly slower switching times than all-solid-state devices. Commonly, measurements are carried out by keeping a constant voltage for prolonged periods of time (around tens of minutes) or by using slow voltage ramp rates (0.1–1 mV s^{-1}). These rather slow parameters amount to several thousands of seconds to complete a single charging/discharging cycle. It is established that the response speed of electrolyte-gated systems can be hampered by the sluggish motion of electrolyte ions.[202] Nonetheless, operating frequencies up to tens of kHz are feasible in electrolyte-gated transistors.[203,204] Thus, faster ME switching speeds may be achievable by employing strategies to optimize the time constant ($\tau = RC$) of the equivalent electrical circuit. This involves an appropriate device engineering

and development of new electrolytes with increased ionic mobility. To date, the fastest ME response in solid/liquid ME composites with on/off modulation of magnetism was achieved in ultrathin films of LSMO gated with DEME-TFSI IL, where repetitive charging/discharging cycles were accomplished in about 10 s.[42]

The nonvolatility of the ME effect is a prerequisite to realize ME memory storage devices. All-solid-state MEs based on ferroelectric/ferromagnetic heterostructures are the most promising candidates to reach this goal. In this respect, the research on solid/liquid MEs has to overcome some nontrivial obstacles. On the one hand, EDL capacitors lack the ability to preserve the stored charge, and so the information carried by magnetic bits is lost once the external voltage is removed. On the other hand, solid/liquid magnetoionics allow for nonvolatility, but at the expense of a reduced switching speed and cycling endurance.

Concerning the areas of sensing and actuation, some promising routes of development were found in relation to the direct ME effect. For instance, all-solid-state laminated composites based on strain-mediated ME coupling are very attractive for the realization of next generation magnetic sensors.[205] Indeed, they allow for the fine detection of magnetic signals, although the issue of noise reduction calls for further improvements. On the front of actuation functionalities, the versatile and precise control of the wireless locomotion of ME nanorobots by means of magnetic fields points out the perspective of using ME effect for therapeutic interventions and drug delivery.[22] In case of the converse ME effect, the areas of sensing and actuation are largely unexplored yet. It has been proposed that strain-coupled laminated composites can be exploited to sense wide range electric fields.[206] Further, albeit the slow switching speed of magnetoionics makes them unsuitable for ME memory applications, their ability to affect bulk magnetic properties under low-voltage conditions shall be convenient for transduction purposes. Moreover, also charge carrier doping, in spite of being predominantly an interface effect, may still operate in the area of sensing and actuation if devices with a conveniently large surface-to-volume ratio, as in the case of porous materials,[43] are employed.

7. Conclusions and Outlook

The present work addresses recent advances in the area of voltage-control of magnetism in all-solid-state and solid/liquid ME composites. Special attention was devoted to the capabilities offered by strain, charge carrier doping, and ionic migration as mediators of the ME effect. A redefinition of the magnetoelectric coupling coefficient $\alpha_{C,V}$ (see Equations 3 and 4), which accounts for the applied voltage rather than the electric field, has been proposed as a new benchmark for the strength of the ME effect, with the aim of facilitating the comparison between different ME systems. Apart from the magnitude of the ME effect, the relevance of other parameters of interest, such as the device lifetime and the switching speed, has been emphasized from the perspective of future applications.

Several are the open challenges yet to be overcome in ME composite systems. Concerning strain-driven effects in all-solid-state ME composites, a concerted effort should be carried out to reduce the applied voltages and improve the device miniaturization. A possible strategy to fulfill both conditions is to identify an appropriate thickness of the piezoelectric component down to a minimum size where strain coupling is still effective. In the case of solid/liquid ME composites, so far, strain coupling has not demonstrated a sufficiently robust ME effect.

Charge carrier doping is at the forefront of the research on MEs. The promising results attained in all-solid-state ME composites, e.g., in ferroelectric/ferromagnetic heterostructures, suggest that several of the envisioned applications in the areas of spintronics and memory storage are gradually progressing toward the point of becoming a practical device reality. In case of solid/liquid ME composites, the full potential of electrostatic and pseudocapacitive charging mechanisms to manipulate magnetism is to be unleashed yet. In particular, the largely unexplored field of ME pseudocapacitors, yielding large ME effect with application of only a few volts, opens new opportunities in the perspective of low-power portable microelectronics.

The newborn field of magnetoionics is growing at a quick pace. On top of the list of quests, there is an urge to enhance the degree of reversibility and the ME response time. In this respect, possible new directions of research shall be pursued by investigating new kinds of ionic carriers. Recently, anion doping via insertion of fluorine ions[207] proved to have a strong impact on the magnetic characteristics of LSMO films. Further, by considering the late achievements in the field of electrochemical batteries, magnesium,[208] sodium,[209] and chloride[210] ions are other interesting candidates to be put in use in magnetoionics.

On the whole, we have described some of the unique features offered by strain, charge, and chemical mechanisms to finely tune the complex interplay between electricity and magnetism at solid/solid and solid/liquid ME interfaces.

Acknowledgements

The authors thank V. Provenzano, R. Witte, S. Dasgupta, X.-L. Ye, R. Singh, B. Breitung, P. M. Leufke, C. Reitz, and R. A. Brand for fruitful discussions. H.H. thanks the Deutsche Forschungsgemeinschaft for financial support under grant number HA 1344/34-1.

Note: Figure 1 was corrected on June 24, 2019, as the color-coded arrows were mislabeled on initial publication online. A missing word in the abstract was also added.

Conflict of Interest

The authors declare no conflict of interest.

Keywords

interface coupling, magnetoelectric effect, magnetoionics, multiferroics, voltage-control of magnetism

Received: October 14, 2018
Revised: December 20, 2018
Published online: February 20, 2019

[1] M. Fiebig, *J. Phys. D: Appl. Phys.* **2005**, *38*, R123.
[2] R. Ramesh, N. Spaldin, *Nat. Mater.* **2007**, *6*, 21.

[3] C. W. Nan, M. I. Bichurin, S. Dong, D. Viehland, G. Srinivasan, *J. Appl. Phys.* **2008**, *103*, 031101.
[4] C. A. F. Vaz, J. Hoffman, C. H. Ahn, R. Ramesh, *Adv. Mater.* **2010**, *22*, 2900.
[5] J. Ma, J. Hu, Z. Li, C.-W. Nan, *Adv. Mater.* **2011**, *23*, 1062.
[6] S. Fusil, V. Garcia, A. Barthélémy, M. Bibes, *Annu. Rev. Mater. Res.* **2014**, *44*, 91.
[7] F. Matsukura, Y. Tokura, H. Ohno, *Nat. Nanotechnol.* **2015**, *10*, 209.
[8] J.-M. Hu, L.-Q. Chen, C.-W. Nan, *Adv. Mater.* **2016**, *28*, 15.
[9] C. Song, B. Cui, F. Li, X. Zhou, F. Pan, *Prog. Mater. Sci.* **2017**, *87*, 33.
[10] P. B. Meisenheimer, S. Novakov, N. M. Vu, J. T. Heron, *J. Appl. Phys.* **2018**, *123*, 240901.
[11] O. O. Brovko, P. Ruiz-Díaz, T. R. Dasa, V. S. Stepanyuk, *J. Phys.: Condens. Matter* **2014**, *26*, 093001.
[12] Y. Wang, J. Hu, Y. Lin, C.-W. Nan, *NPG Asia Mater.* **2010**, *2*, 61.
[13] C. Binek, B. Doudin, *J. Phys.: Condens. Matter* **2005**, *17*, L39.
[14] M. Bibes, A. Barthélémy, *Nat. Mater.* **2008**, *7*, 425.
[15] Z. Zhou, M. Trassin, Y. Gao, Y. Gao, D. Qiu, K. Ashraf, T. Nan, X. Yang, S. R. Bowden, D. T. Pierce, M. D. Stiles, J. Unguris, M. Liu, B. M. Howe, G. J. Brown, S. Salahuddin, R. Ramesh, N. X. Sun, *Nat. Commun.* **2015**, *6*, 6082.
[16] A. B. Ustinov, G. Srinivasan, *Appl. Phys. Lett.* **2008**, *93*, 142503.
[17] S. Dong, J. Zhai, J. F. Li, D. Viehland, S. Priya, *Appl. Phys. Lett.* **2008**, *93*, 103511.
[18] U. Laletsin, N. Padubnaya, G. Srinivasan, C. P. DeVreugd, *Appl. Phys. A* **2004**, *78*, 33.
[19] J. Zhai, Z. Xing, S. Dong, J. Li, D. Viehland, *Appl. Phys. Lett.* **2006**, *88*, 062510.
[20] Z. Chu, H. Shi, M. J. PourhosseiniAsl, J. Wu, W. Shi, X. Gao, X. Yuan, S. Dong, *Sci. Rep.* **2017**, *7*, 8592.
[21] L. A. Dubraja, C. Reitz, L. Velasco, R. Witte, R. Kruk, H. Hahn, T. Brezesinski, *ACS Appl. Nano Mater.* **2018**, *1*, 65.
[22] X.-Z. Chen, M. Hoop, N. Shamsudhin, T. Huang, B. Özkale, Q. Li, E. Siringil, F. Mushtaq, L. Di Tizio, B. J. Nelson, S. Pané, *Adv. Mater.* **2017**, *29*, 1605458.
[23] Unless differently specified, the attribute "converse" is tacitly omitted, since the current work predominantly examines the electric-field control of magnetism.
[24] S. Brivio, D. Petti, R. Bertacco, J. C. Cezar, *Appl. Phys. Lett.* **2011**, *98*, 092505.
[25] G. Venkataiah, Y. Shirahata, M. Itoh, T. Taniyama, *Appl. Phys. Lett.* **2011**, *99*, 102506.
[26] S. Sahoo, S. Polisetty, C.-G. Duan, S. S. Jaswal, E. Y. Tsymbal, C. Binek, *Phys. Rev. B* **2007**, *76*, 092108.
[27] A. Mardana, S. Ducharme, S. Adenwalla, *Nano Lett.* **2011**, *11*, 3862.
[28] U. Bauer, L. Yao, A. J. Tan, P. Agrawal, S. Emori, H. L. Tuller, S. van Dijken, G. S. D. Beach, *Nat. Mater.* **2015**, *14*, 174.
[29] C. Fowley, K. Rode, K. Oguz, H. Kurt, J. M. D. Coey, *J. Phys. D: Appl. Phys.* **2011**, *44*, 305001.
[30] M. Weisheit, S. Fahler, A. Marty, Y. Souche, C. Poinsignon, D. Givord, *Science* **2007**, *315*, 349.
[31] Q. Zhang, X. Luo, L. Wang, L. Zhang, B. Khalid, J. Gong, H. Wu, *Nano Lett.* **2016**, *16*, 583.
[32] A. Quintana, J. Zhang, E. Isarain-Chávez, E. Menéndez, R. Cuadrado, R. Robles, M. D. Baró, M. Guerrero, S. Pané, B. J. Nelson, C. M. Müller, P. Ordejón, J. Nogués, E. Pellicer, J. Sort, *Adv. Funct. Mater.* **2017**, *27*, 1701904.
[33] H. Ohno, D. Chiba, F. Matsukura, T. Omiya, E. Abe, T. Dietl, Y. Ohno, K. Ohtani, *Nature* **2000**, *408*, 944.
[34] D. Chiba, H. Yamanouchi, F. Hatsukura, H. Ohno, *Science* **2003**, *301*, 943.
[35] X. Hong, A. Posadas, A. Lin, H. Ahn, *Phys. Rev. B* **2003**, *68*, 134415.
[36] Y. Yamada, K. Ueno, T. Fukumura, H. T. Yuan, H. Shimotani, Y. Iwasa, L. Gu, S. Tsukimoto, Y. Ikuhara, M. Kawasaki, *Science* **2011**, *332*, 1065.
[37] S. Brivio, M. Cantoni, D. Petti, R. Bertacco, *J. Appl. Phys.* **2010**, *108*, 113906.
[38] H. J. A. Molegraaf, J. Hoffman, C. A. F. Vaz, S. Gariglio, D. van der Marel, C. H. Ahn, J.-M. Triscone, *Adv. Mater.* **2009**, *21*, 3470.
[39] C. A. F. Vaz, Y. Segal, J. Hoffman, R. D. Grober, F. J. Walker, C. H. Ahn, *Appl. Phys. Lett.* **2010**, *97*, 042506.
[40] K. Shimamura, D. Chiba, S. Ono, S. Fukami, N. Ishiwata, M. Kawaguchi, K. Kobayashi, T. Ono, *Appl. Phys. Lett.* **2012**, *100*, 122402.
[41] P. M. Leufke, R. Kruk, R. A. Brand, H. Hahn, *Phys. Rev. B* **2013**, *87*, 094416.
[42] A. Molinari, H. Hahn, R. Kruk, *Adv. Mater.* **2018**, *30*, 1703908.
[43] C. Reitz, D. Wang, D. Stoeckel, A. Beck, T. Leichtweiss, H. Hahn, T. Brezesinski, *ACS Appl. Mater. Interfaces* **2017**, *9*, 22799.
[44] S. Dasgupta, B. Das, Q. Li, D. Wang, T. T. Baby, S. Indris, M. Knapp, H. Ehrenberg, K. Fink, R. Kruk, H. Hahn, *Adv. Funct. Mater.* **2016**, *26*, 7507.
[45] W. Eerenstein, M. Wiora, J. L. Prieto, J. F. Scott, N. D. Mathur, *Nat. Mater.* **2007**, *6*, 348.
[46] R. O. Cherifi, V. Ivanovskaya, L. C. Phillips, A. Zobelli, I. C. Infante, E. Jacquet, V. Garcia, S. Fusil, P. R. Briddon, N. Guiblin, A. Mougin, A. A. Ünal, F. Kronast, S. Valencia, B. Dkhil, A. Barthélémy, M. Bibes, *Nat. Mater.* **2014**, *13*, 345.
[47] Y. Tokunaga, Y. Taguchi, T. Arima, Y. Tokura, *Nat. Phys.* **2012**, *8*, 838.
[48] A. K. Mishra, A. J. Darbandi, P. M. Leufke, R. Kruk, H. Hahn, *J. Appl. Phys.* **2013**, *113*, 033913.
[49] A. Molinari, P. M. Leufke, C. Reitz, S. Dasgupta, R. Witte, R. Kruk, H. Hahn, *Nat. Commun.* **2017**, *8*, 15339.
[50] S. Dasgupta, B. Das, M. Knapp, R. A. Brand, H. Ehrenberg, R. Kruk, H. Hahn, *Adv. Mater.* **2014**, *26*, 4639.
[51] K. Dörr, *J. Phys. D: Appl. Phys.* **2006**, *39*, R125.
[52] J. M. Rondinelli, M. Stengel, N. A. Spaldin, *Nat. Nanotechnol.* **2008**, *3*, 46.
[53] P. Borisov, A. Hochstrat, X. Chen, W. Kleemann, C. Binek, *Phys. Rev. Lett.* **2005**, *94*, 117203.
[54] A. Chen, Y. Zhao, P. Li, X. Zhang, R. Peng, H. Huang, L. Zou, X. Zheng, S. Zhang, P. Miao, Y. Lu, J. Cai, C.-W. Nan, *Adv. Mater.* **2016**, *28*, 363.
[55] S. Jiang, J. Shan, K. F. Mak, *Nat. Mater.* **2018**, *17*, 406.
[56] S. M. Wu, S. A. Cybart, P. Yu, M. D. Rossell, J. X. Zhang, R. Ramesh, R. C. Dynes, *Nat. Mater.* **2010**, *9*, 756.
[57] S. M. Wu, S. A. Cybart, D. Yi, J. M. Parker, R. Ramesh, R. C. Dynes, *Phys. Rev. Lett.* **2013**, *110*, 067202.
[58] M. Liu, Z. Zhou, T. Nan, B. M. Howe, G. J. Brown, N. X. Sun, *Adv. Mater.* **2013**, *25*, 1435.
[59] J. Lou, M. Liu, D. Reed, Y. Ren, N. X. Sun, *Adv. Mater.* **2009**, *21*, 4711.
[60] D. E. Parkes, L. R. Shelford, P. Wadley, V. Holý, M. Wang, A. T. Hindmarch, G. van der Laan, R. P. Campion, K. W. Edmonds, S. A. Cavill, A. W. Rushforth, *Sci. Rep.* **2013**, *3*, 2220.
[61] G. Yu, Z. Wang, M. Abolfath-Beygi, C. He, X. Li, K. L. Wong, P. Nordeen, H. Wu, G. P. Carman, X. Han, I. A. Alhomoudi, P. K. Amiri, K. L. Wang, *Appl. Phys. Lett.* **2015**, *106*, 072402.
[62] P. Hsu, A. Kubetzka, A. Finco, N. Romming, K. von Bergmann, R. Wiesendanger, *Nat. Nanotechnol.* **2016**, *12*, 123.
[63] M. Schott, A. Bernand-Mantel, L. Ranno, S. Pizzini, J. Vogel, H. Béa, C. Baraduc, S. Auffret, G. Gaudin, D. Givord, *Nano Lett.* **2017**, *17*, 3006.
[64] S. Mathews, R. Ramesh, T. Venkatesan, J. Benedetto, *Science* **1997**, *276*, 238.

[65] I. Pallecchi, L. Pellegrino, E. Bellingeri, A. S. Siri, D. Marré, A. Tebano, G. Balestrino, *Phys. Rev. B* **2008**, *78*, 024411.
[66] J. T. Heron, J. L. Bosse, Q. He, Y. Gao, M. Trassin, L. Ye, J. D. Clarkson, C. Wang, J. Liu, S. Salahuddin, D. C. Ralph, D. G. Schlom, J. Íñiguez, B. D. Huey, R. Ramesh, *Nature* **2014**, *516*, 370.
[67] L. M. Zheng, X. R. Wang, W. M. Lü, C. J. Li, T. R. Paudel, Z. Q. Liu, Z. Huang, S. W. Zeng, K. Han, Z. H. Chen, X. P. Qiu, M. S. Li, S. Yang, B. Yang, M. F. Chisholm, L. W. Martin, S. J. Pennycook, E. Y. Tsymbal, J. M. D. Coey, W. W. Cao, *Nat. Commun.* **2018**, *9*, 1897.
[68] H. Schmid, *Ferroelectrics* **1994**, *162*, 317.
[69] D. N. Astrov, *Sov. Phys.-JETP* **1961**, *13*, 729.
[70] V. J. Folen, G. T. Rado, E. W. Stalder, *Phys. Rev. Lett.* **1961**, *6*, 607.
[71] G. Catalan, J. F. Scott, *Adv. Mater.* **2009**, *21*, 2463.
[72] M. Matsubara, S. Manz, M. Mochizuki, T. Kubacka, A. Iyama, N. Aliouane, T. Kimura, S. L. Johnson, D. Meier, M. Fiebig, *Science* **2015**, *348*, 1112.
[73] W. F. Brown, R. M. Hornreich, S. Shtrikman, *Phys. Rev.* **1968**, *168*, 574.
[74] G. T. Rado, V. J. Folen, *Phys. Rev. Lett.* **1961**, *7*, 310.
[75] N. A. Hill, *J. Phys. Chem. B* **2000**, *104*, 6694.
[76] B. D. H. Tellegen, *Phillips Res. Rep.* **1948**, *3*, 81.
[77] C. H. Ahn, A. Bhattacharya, M. Di Ventra, J. N. Eckstein, C. D. Frisbie, M. E. Gershenson, A. M. Goldman, I. H. Inoue, J. Mannhart, A. J. Millis, A. F. Morpurgo, D. Natelson, J.-M. Triscone, *Rev. Mod. Phys.* **2006**, *78*, 1185.
[78] Z. G. Sheng, J. Gao, Y. P. Sun, *Phys. Rev. B* **2009**, *79*, 174437.
[79] J. Jeong, N. Aetukuri, T. Graf, T. D. Schladt, M. G. Samant, S. S. P. Parkin, *Science* **2013**, *339*, 1402.
[80] A. S. Dhoot, C. Israel, X. Moya, N. D. Mathur, R. H. Friend, *Phys. Rev. Lett.* **2009**, *102*, 136402.
[81] K. Ueno, H. Shimotani, Y. Iwasa, M. Kawasaki, *Appl. Phys. Lett.* **2010**, *96*, 252107.
[82] J. Walter, H. Wang, B. Luo, C. D. Frisbie, C. Leighton, *ACS Nano* **2016**, *10*, 7799.
[83] N. A. Spaldin, M. Fiebig, *Science* **2005**, *309*, 391.
[84] L. Suo, O. Borodin, T. Gao, M. Olguin, J. Ho, X. Fan, C. Luo, C. Wang, K. Xu, *Science* **2015**, *350*, 938.
[85] A. Hammami, N. Raymond, M. Armand, *Nature* **2003**, *424*, 635.
[86] L. Hu, K. Xu, *Proc. Natl. Acad. Sci. USA* **2014**, *111*, 3205.
[87] S. Zhang, N. Sun, X. He, X. Lu, X. Zhang, *J. Phys. Chem. Ref. Data* **2006**, *35*, 1475.
[88] K. Ueno, S. Nakamura, H. Shimotani, A. Ohtomo, N. Kimura, T. Nojima, H. Aoki, Y. Iwasa, M. Kawasaki, *Nat. Mater.* **2008**, *7*, 855.
[89] K. Ueno, S. Nakamura, H. Shimotani, H. T. Yuan, N. Kimura, T. Nojima, H. Aoki, Y. Iwasa, M. Kawasaki, *Nat. Nanotechnol.* **2011**, *6*, 408.
[90] K. H. Lee, M. S. Kang, S. Zhang, Y. Gu, T. P. Lodge, C. D. Frisbie, *Adv. Mater.* **2012**, *24*, 4457.
[91] C. Reitz, P. Leufke, R. Schneider, H. Hahn, T. Brezesinski, *Chem. Mater.* **2014**, *26*, 5745.
[92] L. W. Martin, Y.-H. Chu, R. Ramesh, *Mater. Sci. Eng., R* **2010**, *68*, 89.
[93] M. K. Lee, T. K. Nath, C. B. Eom, M. C. Smoak, F. Tsui, *Appl. Phys. Lett.* **2000**, *77*, 3547.
[94] J. Ryu, A. V. Carazo, K. Uchino, H.-E. Kim, *Jpn. J. Appl. Phys.* **2001**, *40*, 4948.
[95] C. Thiele, K. Dörr, O. Bilani, J. Rödel, L. Schultz, *Phys. Rev. B* **2007**, *75*, 054408.
[96] S. Geprägs, D. Mannix, M. Opel, S. T. B. Goennenwein, R. Gross, *Phys. Rev. B* **2013**, *88*, 054412.
[97] J.-W. Lee, S.-C. Shin, S.-K. Kim, *Appl. Phys. Lett.* **2003**, *82*, 2458.
[98] T. H. E. Lahtinen, J. O. Tuomi, S. van Dijken, *Adv. Mater.* **2011**, *23*, 3187.
[99] I. Fina, A. Quintana, J. Padilla-Pantoja, X. Martí, F. Macià, F. Sánchez, M. Foerster, L. Aballe, J. Fontcuberta, J. Sort, *ACS Appl. Mater. Interfaces* **2017**, *9*, 15577.
[100] J. D. Clarkson, I. Fina, Z. Q. Liu, Y. Lee, J. Kim, C. Frontera, K. Cordero, S. Wisotzki, F. Sanchez, J. Sort, S. L. Hsu, C. Ko, L. Aballe, M. Foerster, J. Wu, H. M. Christen, J. T. Heron, D. G. Schlom, S. Salahuddin, N. Kioussis, J. Fontcuberta, X. Marti, R. Ramesh, *Sci. Rep.* **2017**, *7*, 15460.
[101] M. Ghidini, R. Pellicelli, J. L. Prieto, X. Moya, J. Soussi, J. Briscoe, S. Dunn, N. D. Mathur, *Nat. Commun.* **2013**, *4*, 1453.
[102] Y. Shirahata, R. Shiina, D. L. González, K. J. A. Franke, E. Wada, M. Itoh, N. A. Pertsev, S. van Dijken, T. Taniyama, *NPG Asia Mater.* **2015**, *7*, e198.
[103] N. Lei, S. Park, P. Lecoeur, D. Ravelosona, C. Chappert, O. Stelmakhovych, V. Holý, *Phys. Rev. B* **2011**, *84*, 012404.
[104] K. Singh, D. Kaur, *J. Phys. D: Appl. Phys.* **2016**, *49*, 035004.
[105] T. Nan, Z. Zhou, M. Liu, X. Yang, Y. Gao, B. A. Assaf, H. Lin, S. Velu, X. Wang, H. Luo, J. Chen, S. Akhtar, E. Hu, R. Rajiv, K. Krishnan, S. Sreedhar, D. Heiman, B. M. Howe, G. J. Brown, N. X. Sun, *Sci. Rep.* **2015**, *4*, 3688.
[106] H. Zheng, J. Wang, S. E. Lofland, Z. Ma, L. Mohaddes-Ardabili, T. Zhao, L. Salamanca-Riba, S. R. Shinde, S. B. Ogale, F. Bai, D. Viehland, Y. Jia, D. G. Schlom, M. Wuttig, A. Roytburd, R. Ramesh, *Science* **2004**, *303*, 661.
[107] F. Zavaliche, H. Zheng, L. Mohaddes-Ardabili, S. Y. Yang, Q. Zhan, P. Shafer, E. Reilly, R. Chopdekar, Y. Jia, P. Wright, D. G. Schlom, Y. Suzuki, R. Ramesh, *Nano Lett.* **2005**, *5*, 1793.
[108] C. Schmitz-Antoniak, D. Schmitz, P. Borisov, F. M. F. de Groot, S. Stienen, A. Warland, B. Krumme, R. Feyerherm, E. Dudzik, W. Kleemann, H. Wende, *Nat. Commun.* **2013**, *4*, 2051.
[109] L. Yan, M. Zhuo, Z. Wang, J. Yao, N. Haberkorn, S. Zhang, L. Civale, J. Li, D. Viehland, Q. X. Jia, *Appl. Phys. Lett.* **2012**, *101*, 3.
[110] M. Gueye, F. Zighem, D. Faurie, M. Belmeguenai, S. Mercone, *Appl. Phys. Lett.* **2014**, *105*, 052411.
[111] J. Weissmüller, R. N. Viswanath, D. Kramer, P. Zimmer, R. Würschum, H. Gleiter, *Science* **2003**, *300*, 312.
[112] H. Drings, R. N. Viswanath, D. Kramer, C. Lemier, J. Weissmüller, R. Würschum, *Appl. Phys. Lett.* **2006**, *88*, 253103.
[113] C. Lemier, S. Ghosh, R. N. Viswanath, G.-T. Fei, J. Weissmüller, *MRS Proc.* **2005**, *876*, R2.6.
[114] S. Ghosh, C. Lemier, J. Weissmueller, *IEEE Trans. Magn.* **2006**, *42*, 3617.
[115] A. K. Mishra, C. Bansal, M. Ghafari, R. Kruk, H. Hahn, *Phys. Rev. B* **2010**, *81*, 155452.
[116] J. M. D. Coey, M. Viret, S. von Molnár, *Adv. Phys.* **2009**, *58*, 571.
[117] H. Du, X. Lin, Z. Xu, D. Chu, *J. Mater. Sci.* **2015**, *50*, 5641.
[118] B. E. Conway, *J. Electrochem. Soc.* **1991**, *138*, 1539.
[119] B. E. Conway, V. Birss, J. Wojtowicz, *J. Power Sources* **1997**, *66*, 1.
[120] V. Augustyn, P. Simon, B. Dunn, *Energy Environ. Sci.* **2014**, *7*, 1597.
[121] M. R. Lukatskaya, B. Dunn, Y. Gogotsi, *Nat. Commun.* **2016**, *7*, 12647.
[122] D. Choi, G. E. Blomgren, P. N. Kumta, *Adv. Mater.* **2006**, *18*, 1178.
[123] T. Brezesinski, J. Wang, S. H. Tolbert, B. Dunn, *Nat. Mater.* **2010**, *9*, 146.
[124] K.-C. Liu, *J. Electrochem. Soc.* **1996**, *143*, 124.
[125] M. Toupin, T. Brousse, D. Bélanger, *Chem. Mater.* **2004**, *16*, 3184.
[126] S.-C. Pang, M. A. Anderson, T. W. Chapman, *J. Electrochem. Soc.* **2000**, *147*, 444.
[127] P. Ragupathy, D. H. Park, G. Campet, H. N. Vasan, S.-J. Hwang, J.-H. Choy, N. Munichandraiah, *J. Phys. Chem. C* **2009**, *113*, 6303.
[128] J.-K. Chang, M.-T. Lee, W.-T. Tsai, M.-J. Deng, H.-F. Cheng, I.-W. Sun, *Langmuir* **2009**, *25*, 11955.
[129] C. Guan, J. Liu, Y. Wang, L. Mao, Z. Fan, Z. Shen, H. Zhang, J. Wang, *ACS Nano* **2015**, *9*, 5198.
[130] Z. Ren, J. Li, Y. Ren, S. Wang, Y. Qiu, J. Yu, *Sci. Rep.* **2016**, *6*, 20021.

[131] C. Lin, *J. Electrochem. Soc.* **1998**, *145*, 4097.
[132] V. Augustyn, J. Come, M. A. Lowe, J. W. Kim, P.-L. Taberna, S. H. Tolbert, H. D. Abruña, P. Simon, B. Dunn, *Nat. Mater.* **2013**, *12*, 518.
[133] J. T. Mefford, W. G. Hardin, S. Dai, K. P. Johnston, K. J. Stevenson, *Nat. Mater.* **2014**, *13*, 726.
[134] D. Chiba, M. Sawicki, Y. Nishitani, Y. Nakatani, F. Matsukura, H. Ohno, *Nature* **2008**, *455*, 515.
[135] I. Stolichnov, S. W. E. Riester, H. J. Trodahl, N. Setter, A. W. Rushforth, K. W. Edmonds, R. P. Campion, C. T. Foxon, B. L. Gallagher, T. Jungwirth, *Nat. Mater.* **2008**, *7*, 464.
[136] D. Chiba, F. Matsukura, H. Ohno, *Nano Lett.* **2010**, *10*, 4505.
[137] F. Xiu, Y. Wang, J. Kim, A. Hong, J. Tang, A. P. Jacob, J. Zou, K. L. Wang, *Nat. Mater.* **2010**, *9*, 337.
[138] T. Maruyama, Y. Shiota, T. Nozaki, K. Ohta, N. Toda, M. Mizuguchi, A. A. Tulapurkar, T. Shinjo, M. Shiraishi, S. Mizukami, Y. Ando, Y. Suzuki, *Nat. Nanotechnol.* **2009**, *4*, 158.
[139] D. Chiba, S. Fukami, K. Shimamura, N. Ishiwata, K. Kobayashi, T. Ono, *Nat. Mater.* **2011**, *10*, 853.
[140] A. J. Schellekens, A. van den Brink, J. H. Franken, H. J. M. Swagten, B. Koopmans, *Nat. Commun.* **2012**, *3*, 847.
[141] D. Chiba, M. Kawaguchi, S. Fukami, N. Ishiwata, K. Shimamura, K. Kobayashi, T. Ono, *Nat. Commun.* **2012**, *3*, 888.
[142] W.-G. Wang, M. Li, S. Hageman, C. L. Chien, *Nat. Mater.* **2012**, *11*, 64.
[143] Y. Shiota, T. Nozaki, F. Bonell, S. Murakami, T. Shinjo, Y. Suzuki, *Nat. Mater.* **2012**, *11*, 39.
[144] X. Hong, A. Posadas, C. H. Ahn, *Appl. Phys. Lett.* **2005**, *86*, 142501.
[145] T. Kanki, H. Tanaka, T. Kawai, *Appl. Phys. Lett.* **2006**, *89*, 242506.
[146] H. Lu, T. A. George, Y. Wang, I. Ketsman, J. D. Burton, C.-W. Bark, S. Ryu, D. J. Kim, J. Wang, C. Binek, P. A. Dowben, A. Sokolov, C.-B. Eom, E. Y. Tsymbal, A. Gruverman, *Appl. Phys. Lett.* **2012**, *100*, 232904.
[147] D. Yi, J. Liu, S. Okamoto, S. Jagannatha, Y.-C. Chen, P. Yu, Y.-H. Chu, E. Arenholz, R. Ramesh, *Phys. Rev. Lett.* **2013**, *111*, 127601.
[148] M. K. Niranjan, J. D. Burton, J. P. Velev, S. S. Jaswal, E. Y. Tsymbal, *Appl. Phys. Lett.* **2009**, *95*, 052501.
[149] M. K. Niranjan, J. P. Velev, C. G. Duan, S. S. Jaswal, E. Y. Tsymbal, *Phys. Rev. B* **2008**, *78*, 104405.
[150] A. J. Grutter, B. J. Kirby, M. T. Gray, C. L. Flint, U. S. Alaan, Y. Suzuki, J. A. Borchers, *Phys. Rev. Lett.* **2015**, *115*, 047601.
[151] C. A. F. Vaz, J. Hoffman, Y. Segal, J. W. Reiner, R. D. Grober, Z. Zhang, C. H. Ahn, F. J. Walker, *Phys. Rev. Lett.* **2010**, *104*, 127202.
[152] L. Jiang, W. S. Choi, H. Jeen, S. Dong, Y. Kim, M.-G. Han, Y. Zhu, S. V. Kalinin, E. Dagotto, T. Egami, H. N. Lee, *Nano Lett.* **2013**, *13*, 5837.
[153] S. Zhao, Z. Zhou, B. Peng, M. Zhu, M. Feng, Q. Yang, Y. Yan, W. Ren, Z.-G. Ye, Y. Liu, M. Liu, *Adv. Mater.* **2017**, *29*, 1606478.
[154] E. Dislaki, S. Robbennolt, M. Campoy-Quiles, J. Nogués, E. Pellicer, J. Sort, *Adv. Sci.* **2018**, *5*, 1800499.
[155] M. Endo, D. Chiba, H. Shimotani, F. Matsukura, Y. Iwasa, H. Ohno, *Appl. Phys. Lett.* **2010**, *96*, 022515.
[156] H. Kuang, J. Wang, F. X. Hu, Y. Y. Zhao, Y. Liu, R. R. Wu, J. R. Sun, B. G. Shen, *Appl. Phys. Lett.* **2016**, *108*, 082407.
[157] J. Lourembam, J. Wu, J. Ding, W. Lin, T. Wu, *Phys. Rev. B* **2014**, *89*, 014425.
[158] T. Hatano, Z. Sheng, M. Nakamura, M. Nakano, M. Kawasaki, Y. Iwasa, Y. Tokura, *Adv. Mater.* **2014**, *26*, 2874.
[159] L. Zhang, W. Hou, G. Dong, Z. Zhou, S. Zhao, Z. Hu, W. Ren, M. Chen, C. Nan, J. Ma, H. Zhou, W. Chen, Z.-G. Ye, Z. Jiang, M. Liu, *Mater. Horiz.* **2018**, *5*, 991.
[160] S. Topolovec, P. Jerabek, D. V. Szabó, H. Krenn, R. Würschum, *J. Magn. Magn. Mater.* **2013**, *329*, 43.
[161] C. Bi, Y. Liu, T. Newhouse-Illige, M. Xu, M. Rosales, J. W. Freeland, O. Mryasov, S. Zhang, S. G. E. te Velthuis, W. G. Wang, *Phys. Rev. Lett.* **2014**, *113*, 267202.
[162] D. A. Gilbert, A. J. Grutter, E. Arenholz, K. Liu, B. J. Kirby, J. A. Borchers, B. B. Maranville, *Nat. Commun.* **2016**, *7*, 12264.
[163] A. J. Grutter, D. A. Gilbert, U. S. Alaan, E. Arenholz, B. B. Maranville, J. A. Borchers, Y. Suzuki, K. Liu, B. J. Kirby, *Appl. Phys. Lett.* **2016**, *108*, 082405.
[164] X. Zhu, J. Zhou, L. Chen, S. Guo, G. Liu, R.-W. Li, W. D. Lu, *Adv. Mater.* **2016**, *28*, 7658.
[165] G. Wei, L. Wei, D. Wang, Y. Chen, Y. Tian, S. Yan, L. Mei, J. Jiao, *Appl. Phys. Lett.* **2017**, *110*, 062404.
[166] C. Reitz, C. Suchomski, D. Wang, H. Hahn, T. Brezesinski, *J. Mater. Chem. C* **2016**, *4*, 8889.
[167] T. Yamada, K. Morita, K. Kume, H. Yoshikawa, K. Awaga, *J. Mater. Chem. C* **2014**, *2*, 5183.
[168] G. Wei, L. Wei, D. Wang, Y. Chen, Y. Tian, S. Yan, L. Mei, J. Jiao, *Sci. Rep.* **2017**, *7*, 12554.
[169] G. Klinser, S. Topolovec, H. Kren, S. Koller, W. Goessler, H. Krenn, R. Würschum, *Appl. Phys. Lett.* **2016**, *109*, 213901.
[170] G. Klinser, M. Stückler, H. Kren, S. Koller, W. Goessler, H. Krenn, R. Würschum, *J. Power Sources* **2018**, *396*, 791.
[171] K. Taniguchi, K. Narushima, H. Sagayama, W. Kosaka, N. Shito, H. Miyasaka, *Adv. Funct. Mater.* **2017**, *27*, 1604990.
[172] K. Duschek, D. Pohl, S. Fähler, K. Nielsch, K. Leistner, *APL Mater.* **2016**, *4*, 032301.
[173] K. Duschek, A. Petr, J. Zehner, K. Nielsch, K. Leistner, *J. Mater. Chem. C* **2018**, *6*, 8411.
[174] K. Leistner, J. Wunderwald, N. Lange, S. Oswald, M. Richter, H. Zhang, L. Schultz, S. Fähler, *Phys. Rev. B* **2013**, *87*, 224411.
[175] L. Reichel, S. Oswald, S. Fähler, L. Schultz, K. Leistner, *J. Appl. Phys.* **2013**, *113*, 143904.
[176] B. Cui, C. Song, G. Wang, Y. Yan, J. Peng, J. Miao, H. Mao, F. Li, C. Chen, F. Zeng, F. Pan, *Adv. Funct. Mater.* **2014**, *24*, 7233.
[177] C. Ge, K.-J. Jin, L. Gu, L.-C. Peng, Y.-S. Hu, H.-Z. Guo, H.-F. Shi, J.-K. Li, J.-O. Wang, X.-X. Guo, C. Wang, M. He, H.-B. Lu, G.-Z. Yang, *Adv. Mater. Interfaces* **2015**, *2*, 1500407.
[178] J. Walter, G. Yu, B. Yu, A. Grutter, B. Kirby, J. Borchers, Z. Zhang, H. Zhou, T. Birol, M. Greven, C. Leighton, *Phys. Rev. Mater.* **2017**, *1*, 071403.
[179] H. T. Yi, B. Gao, W. Xie, S.-W. Cheong, V. Podzorov, *Sci. Rep.* **2015**, *4*, 6604.
[180] A. Quintana, E. Menéndez, M. O. Liedke, M. Butterling, A. Wagner, V. Sireus, P. Torruella, S. Estradé, F. Peiró, J. Dendooven, C. Detavernier, P. D. Murray, D. A. Gilbert, K. Liu, E. Pellicer, J. Nogues, J. Sort, *ACS Nano* **2018**, *12*, 10291.
[181] N. Lu, P. Zhang, Q. Zhang, R. Qiao, Q. He, H.-B. Li, Y. Wang, J. Guo, D. Zhang, Z. Duan, Z. Li, M. Wang, S. Yang, M. Yan, E. Arenholz, S. Zhou, W. Yang, L. Gu, C.-W. Nan, J. Wu, Y. Tokura, P. Yu, *Nature* **2017**, *546*, 124.
[182] Y. N. Yan, X. J. Zhou, F. Li, B. Cui, Y. Y. Wang, G. Y. Wang, F. Pan, C. Song, *Appl. Phys. Lett.* **2015**, *107*, 122407.
[183] B. Cui, C. Song, F. Li, X. Y. Zhong, Z. C. Wang, P. Werner, Y. D. Gu, H. Q. Wu, M. S. Saleem, S. S. P. Parkin, F. Pan, *Phys. Rev. Appl.* **2017**, *8*, 044007.
[184] Y. T. Liu, S. Ono, G. Agnus, J.-P. Adam, S. Jaiswal, J. Langer, B. Ocker, D. Ravelosona, L. Herrera Diez, *J. Appl. Phys.* **2017**, *122*, 133907.
[185] A. Obinata, Y. Hibino, D. Hayakawa, T. Koyama, K. Miwa, S. Ono, D. Chiba, *Sci. Rep.* **2015**, *5*, 14303.
[186] A. Herklotz, E.-J. Guo, A. T. Wong, T. L. Meyer, S. Dai, T. Z. Ward, H. N. Lee, M. R. Fitzsimmons, *Nano Lett.* **2017**, *17*, 1665.
[187] F. Bi, M. Huang, S. Ryu, H. Lee, C.-W. Bark, C.-B. Eom, P. Irvin, J. Levy, *Nat. Commun.* **2014**, *5*, 5019.

[188] H. Ueda, T. Akita, Y. Uchida, T. Kimura, *Appl. Phys. Lett.* **2017**, *111*, 262901.
[189] A. Mertelj, N. Osterman, D. Lisjak, M. Čopič, *Soft Matter* **2014**, *10*, 9065.
[190] K. Suzuki, Y. Uchida, R. Tamura, Y. Noda, N. Ikuma, S. Shimono, J. Yamauchi, *Soft Matter* **2013**, *9*, 4687.
[191] A. Fert, V. Cros, J. Sampaio, *Nat. Nanotechnol.* **2013**, *8*, 152.
[192] S. S. P. Parkin, M. Hayashi, L. Thomas, *Science* **2008**, *320*, 190.
[193] L. F. Henrichs, O. Cespedes, J. Bennett, J. Landers, S. Salamon, C. Heuser, T. Hansen, T. Helbig, O. Gutfleisch, D. C. Lupascu, H. Wende, W. Kleemann, A. J. Bell, *Adv. Funct. Mater.* **2016**, *26*, 2111.
[194] J. Wang, J. Ma, Z. Li, Y. Shen, Y. Lin, C. W. Nan, *J. Appl. Phys.* **2011**, *110*, 043919.
[195] V. Laukhin, V. Skumryev, X. Martì, D. Hrabovsky, F. Sànchez, M. V. Garcìa-Cuenca, C. Ferrater, M. Varela, U. Lüders, J. F. Bobo, J. Fontcuberta, *Phys. Rev. Lett.* **2006**, *97*, 227201.
[196] A. Moreo, S. Yunoki, E. Dagotto, *Science* **1999**, *283*, 2034.
[197] T. Becker, C. Streng, Y. Luo, V. Moshnyaga, B. Damaschke, N. Shannon, K. Samwer, *Phys. Rev. Lett.* **2002**, *89*, 237203.
[198] S. Couet, M. Bisht, M. Trekels, M. Menghini, C. Petermann, M. J. Van Bael, J. P. Locquet, R. Rüffer, A. Vantomme, K. Temst, *Adv. Funct. Mater.* **2014**, *24*, 71.
[199] A. G. Pandolfo, A. F. Hollenkamp, *J. Power Sources* **2006**, *157*, 11.
[200] J. Hoffman, X. Hong, C. H. Ahn, *Nanotechnology* **2011**, *22*, 254014.
[201] J. M. Hu, T. Yang, J. Wang, H. Huang, J. Zhang, L. Q. Chen, C. W. Nan, *Nano Lett.* **2015**, *15*, 616.
[202] H. Yuan, H. Shimotani, A. Tsukazaki, A. Ohtomo, M. Kawasaki, Y. Iwasa, *Adv. Funct. Mater.* **2009**, *19*, 1046.
[203] J. H. Cho, J. Lee, Y. He, B. Kim, T. P. Lodge, C. D. Frisbie, *Adv. Mater.* **2008**, *20*, 686.
[204] J. H. Cho, J. Lee, Y. Xia, B. Kim, Y. He, M. J. Renn, T. P. Lodge, C. D. Frisbie, *Nat. Mater.* **2008**, *7*, 900.
[205] Y. J. Wang, J. F. Li, D. Viehland, *Mater. Today* **2014**, *17*, 269.
[206] F. Xue, J. Hu, S. X. Wang, J. He, *Appl. Phys. Lett.* **2015**, *106*, 082901.
[207] P. A. Sukkurji, A. Molinari, C. Reitz, R. Witte, C. Kübel, V. S. K. Chakravadhanula, R. Kruk, O. Clemens, *Materials* **2018**, *11*, 1204.
[208] Z. Zhao-Karger, M. Fichtner, *MRS Commun.* **2017**, *7*, 770.
[209] P. Gao, C. Wall, L. Zhang, M. A. Reddy, M. Fichtner, *Electrochem. Commun.* **2015**, *60*, 180.
[210] X. Zhao, S. Ren, M. Bruns, M. Fichtner, *J. Power Sources* **2014**, *245*, 706.
[211] C. H. Ahn, J.-M. Triscone, J. Mannhart, *Nature* **2003**, *424*, 1015.
[212] N. P. Maity, R. Maity, R. K. Thapa, S. Baishya, *Adv. Mater. Sci. Eng.* **2014**, *2014*, 1.
[213] D. Wei, T. Hossain, N. Y. Garces, N. Nepal, H. M. Meyer, M. J. Kirkham, C. R. Eddy, J. H. Edgar, *ECS J. Solid State Sci. Technol.* **2013**, *2*, N110.
[214] K. J. Choi, M. Biegalski, Y. L. Li, A. Sharan, J. Schubert, R. Uecker, P. Reiche, Y. B. Chen, X. Q. Pan, V. Gopalan, L. Q. Che, D. C. Schlom, C. B. Eom, *Science* **2004**, *306*, 1005.
[215] S. W. Choi, R. T. R. Shrout, S. J. Jang, A. S. Bhalla, *Ferroelectrics* **1989**, *100*, 29.
[216] P. M. Leufke, R. Kruk, D. Wang, C. Kübel, H. Hahn, *AIP Adv.* **2012**, *2*, 032184.
[217] H. Ji, X. Zhao, Z. Qiao, J. Jung, Y. Zhu, Y. Lu, L. L. Zhang, A. H. MacDonald, R. S. Ruoff, *Nat. Commun.* **2014**, *5*, 3317.
[218] H. Shimotani, H. Asanuma, A. Tsukazaki, A. Ohtomo, M. Kawasaki, Y. Iwasa, *Appl. Phys. Lett.* **2007**, *91*, 082106.
[219] U. Bauer, S. Emori, G. S. D. Beach, *Nat. Nanotechnol.* **2013**, *8*, 411.